Technical reference for

The Extrapolating Logarithmic Flow (ELF) Model

– An operational low flow forecasting system for British Columbia

Charles Luo, Ph.D., P.Eng.

(Koksilah River, June 18, 2019)

A technical report of the BC River Forecast Centre
Victoria, British Columbia, Canada
August 2023

Abstract

British Columbia (BC) experienced and is experiencing drought hazards, and the River Forecast Centre (RFC) is part of BC provincial drought responding resources. Extreme low flows may pose hydrological and/or ecological drought hazards. On this background, the Extrapolating Logarithmic Flow (ELF) Model was developed in the RFC for medium-term low flow forecasting for BC watersheds. The ELF Model is a mathematical/empirical model, which uses 30-day flow data of discharges and water levels as input to produce 30-day low flow forecasts of discharges and water levels, which are analogues to ensemble forecasts.

In this study, the low flow is redefined from the hydrological perspective, which makes the low flow more predictable under climate change scenarios. Based on this definition, the major characteristic of low flow is summarized as that the streamflow is decreasing, and the rate of decreasing becomes smaller and smaller with time. To avoid the obstacles faced by hydrological methods in low flow simulation, this study employs a mathematical or empirical method to forecast low flows. The fundamental assumption for mathematical methods for low flow forecasting is that the sum of the water release rate from the watershed liquid water storage plus the net meteorological liquid water input rate to the streamflow is a function of time and parameters, and the parameters remain constant for a certain period.

The basic equation for the mathematical method for low flow forecasting in this study is the exponential recession equation. However, the actual low flow data may include significant noises, and the logarithmic flow may not always be linear. In this study, the so-called “twelve-step and twelve-scenario scheme” is developed to meet the challenges posed by the data noise and non-linear logarithmic flow issues. This scheme also produces analogues to ensemble forecasts for low flows, which include forecast maximums, minimums, and averages for the next 30 days.

In this study, a different approach is employed to evaluate the model forecast accuracy – how the forecast maximums and minimums accommodate the observed flows. The ELF Model was put into operation as of July 2018 and together with the reconstructed “forecasts” from January 2015 to June 2018, there is a total of 8 years of forecasts to the end of 2022 (about 800) for each of the 439 stations. A statistical analysis for the ELF Model historical forecasts for all the flow stations was carried out, and the results show that, in general, the ELF Model has better forecasts for most stations in July and August than in the other months, the model forecast accuracy is the lowest in April and May, and the model forecast accuracy for water levels is higher than that for discharges.

Table of Contents

List of Tables

List of Figures

1. Introduction

Most regions of Canada have periods of drought in the hydrological year, but drought hazards are more frequent in the Prairies and interior of British Columbia (BC) due to their geographic locations, which are separated from the Pacific Ocean by the coastal mountains that serve as natural barriers to the transportation of air moisture or precipitation from the coasts. In the past two centuries, several long-duration droughts have occurred in BC and other parts of western Canada (Bonsal et al., 2011).

Although the number of consecutive days without measurable precipitation was decreasing in BC (Vincent and Mekis, 2006) from 1950 to 2007, it was found that the summer mean maximum temperatures have significantly increased over most parts of Canada, especially in the west including BC and the Prairies (Mekis and Vincent, 2008). Extreme summer temperatures are connected to historical droughts, e.g., 1936, 1937, 1961, 1984, 1985, 1988, 2001 and 2002 (Mekis and Vincent, 2008).

The 2015 drought may be the worst one in the recent memory, starting with lower-than-normal snowpacks. Drought levels ramped up quickly for much of southern BC to Level 4, which was the highest drought response level on the provincial rating scale in the years before 2021, due to hot and dry conditions in late August (BC Gov., 2023 a). Several extreme-low streamflow advisories and extreme wildfire risk ratings were issued. Stringent water restrictions were in place by the end of June as some of the rivers reached their lowest records since measurements began 80 to 100 years ago (Szeto et al., 2016). In 2018, it was unusual that the entire coast including the Northwest, which did not normally experience drought in the history, was impacted by severe drought of the highest Level (Level 4) that prevailed late into November (BC Gov., 2023 a).

The spring of 2021 started with dry and seasonal temperatures in most regions of BC, which continued throughout May and June. At the end of June a "heat dome" event," which was an unprecedentedly extreme high temperature over 40 ^{o}C for most parts of the province, triggering significant snowmelt and glacier melt. Drought conditions were significantly worsened for Vancouver Island, the South Coast, and the Southern Interior by mid-July and intensified into August and September with several streams falling below the "critical environmental flow thresholds" for several weeks for these regions (BC Gov., 2023 a).

In 2022, drought extended into December due to prolonged precipitation deficits starting in the summer, with Levels 4 and 5 for the northeast. In a communication in early August 2023, provincial officials stated that the 2023 drought and wildfire situations in BC are also unprecedented, which were caused by early and rapid snowmelt in May 2023 and continuous lack of precipitation across much of the province in the summer.

To facilitate drought management across BC, the "British Columbia Drought Response Plan" (Econnics and MOE, 2015) and the new version titled "British Columbia Drought and Water Scarcity Response Plan" (WLRS and IADWG, 2023) (hereinafter referred to as "the Plan") were developed. In the Plan, drought is defined as "a recurrent feature of climate involving a deficiency of precipitation over an extended period, resulting in a water shortage for activities, communities or aquatic ecosystems." In BC, drought may be caused by combinations of insufficient snow accumulation, hot and dry weather and/or delay in rainfall. From the perspective of its impacts, drought can be meteorological, hydrological, agricultural, socio-economical or ecological. Hydrological drought is formed when the water levels in rivers, reservoirs, lakes and aquifers fall below certain thresholds, resulting in water scarcity and affecting the ecosystems, hydroelectric power generation, and recreational, industrial and urban water use, and BC's First Nations water values (Econnics and MOE, 2015; WLRS and IADWG, 2023).

In Appendix 4 of the Plan, "Provincial Agencies/ Ministry of Forests (FOR)" under "Provincial and Federal Agency Drought Responsibilities" reads, "Operates the River Forecast Centre; collects and interprets snow, meteorological and stream flow data to provide warnings and forecasts of stream and lake runoff conditions." (WLRS and IADWG, 2023). In Appendix 7 of the Plan, "Provincial Government Resources/ River Forecast Centre (RFC)" under "Additional Resources" reads, "The RFC collects and interprets snow, meteorological and stream flow data to provide warnings and forecasts of stream and lake runoff conditions around the province." (WLRS and IADWG, 2023). In simple words, the RFC is part of the drought management resources of BC, and low flow forecasting for drought managements is within its responsibilities. In a communication between the branch management and the RFC modelers in early 2018, developing a low flow forecast model in the RFC was first discussed. On this background, a medium lead time (30 days) low flow forecasting model – the Extrapolating Logarithmic Flow (ELF) Model was developed in the RFC.

Drought is a natural event resulting from less than normal precipitation and above normal temperatures for an extended period, while the low flow is a seasonal phenomenon of any river which may occur in any year. This means that droughts include low flow periods even though a continuous seasonal low flow event does not necessarily constitute a drought. Yet, many researchers referred to a continuous low flow period in year as an annual drought (Smakhtin, 2001). Therefore, low flow forecasting is important for drought managements and responses.

However, low flow simulation and forecasting remains a difficult task for hydrological modellers because the low flow is a long-lasting phenomenon with slow dynamics comparing to floods (Nicolle, et al., 2014). Nicolle, et al. (2014) tested five traditional hydrological models, four conceptual lumped-sum models and one physically based distributed model, in 21 French watersheds, and they found that the forecasts are good only for a short lead time (7 days). Demirel et al. (2015) investigated the ability of two conceptual hydrological models and one data-driven model based on Artificial Neural Networks (ANNs) for low flow forecasts in the Moselle River for a lead time of 90 days, using ensemble seasonal meteorological forecasts as input. It was found that all the models systematically overestimated the runoff during low flow periods, and all the models underestimated the low flows beyond 90 days in the very dry year of 2003 without precipitation data input.

On the other hand, empirical methods for low flow forecasting have been developed long before the conceptual lumped modeling and physically based modeling. Barnes (1939) noticed the recession characteristics of the streamflow when he plotted the low flow on semi-logarithmic papers, which showed a roughly straight line. Based on this finding, researchers have summarized a few forms of the recession equation for the low flow (e.g. Toebes and Strang, 1964; Hall, 1968; Reed and Warne, 1985). However, due to low computing capability and lack of automatic data entry, the early empirical models for low flow forecasting were only able to forecast a very short lead time, such as 2 days (Reed and Warne, 1985). Risva et al. (2018) provided a simple model for low flow forecasting in the Mediterranean region for a lead time up to six months, and the core of their methodology is the exponential recession function. In their model, Risva et al. (2018) used the low flow data from the previous years to calibrate the model to determine the recession parameter, and the low flow period was preset to a six-month period from April 15 to October 15. The preset low flow period limits their model's applicability in a fast-changing climate.

Moreover, when the actual low flow data from a large number of flow stations (more than 400) in BC were studied by the author of this study, it was found the actual low flow data may include significant data noises stemmed from rainfall and/or snow melts and/or measurement errors. Meanwhile, the actual low flow may not strictly follow the trend of the exponential recession equation. These data issues posed significant challenges to low flow forecasting. In the ELF Model, which is a mathematical (empirical) model employing the exponential recession equation in the form presented by Reed and Warne (1985) as the basic governing equation, a special numerical scheme, the so-called "twelve-step and twelve-scenario scheme" was developed. This scheme not only is able to meet the challenges posed by the above data issues, but also produces analogues to ensemble forecasts. In this study, the ELF Model uses 30-day observed daily flow data of discharges and/or water levels to produce 30-day forecasts of discharges and/or water levels at a daily time interval. The model can be run all year round which does not require a preset period of low flow or dry season.

In the coming sections, starting from the definition of low flow from the hydrological perspective, the characteristics of low flow are reviewed, and the obstacles of low flow simulation with hydrological methods are discussed. After the fundamental assumption for mathematical methods for low flow simulation is laid out, the basic equation of the mathematical method is given, and solution of the exponential recession equation for an overdetermined system is derived. Flow data issues for low flow simulation are discussed briefly, and then the "twelve-step and twelve-scenario scheme" is depicted in detail. The method for the EFL Model historical forecast accuracy evaluation is related, and the results of the statistical analysis are presented. At the end of this technical report, this study is summarized and concluded.

2. Definition and characteristics of low flow from hydrological perspective

In the document titled “Definition and Characteristics of Low Flows” (USEPA, 2022), Section “What is low flow?” reads, “Low flow is the ‘flow of water in a stream during prolonged dry weather’ according to the World Meteorological Organization. Many states use design flow statistics such as the 7Q10 (the lowest 7-day average flow that occurs on average once every 10 years) to define low flow for setting permit discharge limits.” This definition of low flow is more or less from the perspective of water supply and environmental management. Moreover, according to USEPA (2022), any year can be an anomaly with respect to occurrence and time of occurrence of low flows, and the magnitude and duration of low flows can vary significantly from year to year. This statement points out the highly unpredictable nature of low flows.

World Meteorological Organization (WMO)’s Manual on Low flow Estimation and Prediction (WMO, 2008) gives the causes of low flow as, (a) an extended dry period leading to a climatic water deficit when potential evaporation exceeds precipitation, or (b) extended periods of low temperatures during which precipitation is stored as snow. WMO (2008) also describes the geological and geomorphological factors of a watershed that affect the process of low flow.

Starting from the concepts given above, the low flow is re-defined from the hydrological perspective in this study so that the low flow is more predictable. If a single watershed is examined as an isolated geomorphological body, the liquid water storage S in the watershed can be written as

$$S = S_f + S_s + S_g \tag{1}$$

in which S_f is the surface water, S_s is the soil moisture, and S_g is the groundwater. The change of water storage dS can be written as

$$dS = d(S_f + S_s + S_g) = [(R + M - E)A - Q]dt \tag{2}$$

where, R is the watershed averaged rainfall rate, M is the watershed averaged rate of snowmelt and/or glacier melt, E is the watershed averaged actual rate of evapotranspiration, A is the watershed area, and Q is the outflow from the watershed (discharge at the outlet). Rearranging Equation (2), it becomes

$$Q = (-\frac{dS}{dt}) + (R + M - E)A \tag{3}$$

Or

$$Q = \Phi + \Psi \tag{4}$$

where $\Phi = -ds/dt$, which is the water release rate from the watershed liquid water storage, and $\Psi =$

$(R + M - E)A$, which is the net meteorological liquid water input rate to the watershed.

From Equations (3) and (4), it can be seen that there are two sources of the outflow Q of the watershed, (i) the direct release from the liquid water storage of the watershed, which is the first term of Equations (3) and (4), including the releases from the surface water and groundwater (the soil moisture can not directly release to the streamflow); (ii) the net meteorological liquid water input, which is the second term of Equations (3) and (4), including rainfall and snowmelt/glacier melt subtracting evapotranspiration.

In order to investigate the change of Q with time, time derivative calculation is carried out on both sides of Equation (4)

$$\frac{dQ}{dt} = \frac{d}{dt}(\Phi + \Psi) \tag{5}$$

Multiplying dt to both sides of Equation (5), it becomes

$$dQ = d(\Phi + \Psi) \tag{6}$$

Discretizing Equation (6) into the differential form, it can be written as

$$\Delta Q = \Delta(\Phi + \Psi) \tag{7}$$

For time step t and t+1

$$Q_{t+1} - Q_t = (\Phi_{t+1} + \Psi_{t+1}) - (\Phi_t + \Psi_t) \tag{8}$$

When the outflow Q from the watershed is observed decreasing ($Q_{t+1} - Q_t < 0$), and from Equation (4) it is noticed that $\Phi_t + \Psi_t = Q_t$, the following equation can be derived from Equation (8)

$$\begin{cases} \Phi_{t+1} + \Psi_{t+1} < Q_t \\ Q_{t+1} - Q_t < 0 \end{cases} \tag{9}$$

The physical meaning of Equation (9) is that the outflow Q from the watershed starts decreasing when the sum of the rate of release from the watershed liquid water storage (Φ) plus the rate of net meteorological liquid water input (Ψ) is smaller than the outflow. The low flow in this study will be defined based on Equation (9).

Definition: The low flow is the outflow from a watershed that has been continuously decreasing from the most recent high peak for a period (T_0):

$$\begin{cases} \Delta Q = \Delta(\Phi + \Psi) < 0 \\ Q_L = Q_t, \qquad \text{when } t \geq T_0 \end{cases} \tag{10}$$

in which Q_L is the low flow, and T_0 is the so-called receding period in this study.

From the above definition and Equations (3) to (10), the characteristics of low flow can be summarized as follows,

a. The streamflow is decreasing.
b. The sum of the rate of release from the watershed liquid water storage plus the rate of net meteorological liquid water input to the watershed is decreasing.
c. The net meteorological liquid water input to the watershed is not sufficient to replenish the liquid water storage in the watershed so that the flow continues to decrease.
d. It can be inferred from c that the watershed liquid water storage is decreasing.

In order to determine the receding period (T_0), this study recommends that the "recent high peak" is a peak equal to or larger than 2 times of the mean annual discharge (MAD), "continuously decreasing" may not be strictly fulfilled and minor rises smaller than 1/2 MAD can be neglected, and "for a period" is the time from the "recent high peak" until the streamflow reaches 1/2 MAD.

Table 1 lists the average receding periods ($\overline{T_0}$) for 10 coastal watersheds and 10 interior watersheds calculated from the resent 10 years of daily streamflow data from Water Survey of Canada (WSC). In Table 1, A is the watershed area, SQRT(A) is the square root of the watershed area, MAD is the mean annual discharge, $\overline{T_0}$ is the average receding period, and WTS is the abbreviation of watershed. From Table 1, it can be seen that the receding periods for the interior watersheds are significantly longer than those for the coastal watersheds because most of streamflow peaks in the coastal watersheds are storm triggered and most of peaks in the interior watersheds are snowmelt dominated.

The above definition of low flow makes the low flow to be more predictable under climate change, without presetting a low flow period or predefining a threshold as long as the average receding period is determined with the historical flow data. For example, the watershed of TOFINO CREEK NEAR THE MOUTH (08HB086) has been experiencing more and more summer rain or storms during the dry season from July to August in recent years due to climate change. If it cannot be said that the entire July and August is the low flow or dry season, it can be said that the streamflow will drop back to the low flow regime approximately 3 days after a rainfall event or storm according to the average receding period given in Table 1. For the watershed of FRASER RIVER AT HOPE (08MF005), the annual peak may occur in any month of May, June or July, and it can be predicted that the low flow period will arrive about 100 days after the streamflow peaks based on the average receding period given in Table 1.

Figure 1 shows two extreme examples of the receding period T_0 , the TOFINO CREEK NEAR THE MOUTH (08HB086) (A = 38.6 km^2), for which $T_0 =$ 2.3 to 3.2 days for a period from December 21, 2022 to January 20, 2023, and the FRASER RIVER AT HOPE (08MF005) (A = 217,000 km^2), for which $T_0 = 96$ days in 2022. Figure 2 shows the linear correlations between the average receding period $\overline{T_0}$ and the square root of watershed area for the 10 coastal watersheds and 10 interior watersheds listed in Tabel 1, respectively. It can be seen from Figure 2 that the average receding period $\overline{T_0}$ is linearly correlated to the square root of watershed area with an R squared larger than 0.8 for both types of watersheds.

Table 1. Average receding periods ($\overline{T_0}$) for 10 coastal watersheds and 10 interior watersheds.

STATION ID	STATION NAME	A (km^2)	SQRT(A) (km)	MAD (m^3/s)	½ MAD (m^3/s)	$\overline{T_0}$ (days)	WTS
08HB086	TOFINO CREEK NEAR THE MOUTH	38.6	6.2	6.8	3.4	3	COASTAL
08GB013	CLOWHOM RIVER NEAR CLOWHOM LAKE	147	12.1	15.4	7.7	5	COASTAL
08MH147	STAVE RIVER ABOVE STAVE LAKE	290	17.0	34.5	17.2	5	COASTAL
08GF007	WAKEMAN RIVER BELOW ATWAYKELLESSE RIVER	698	26.4	78.1	39.1	5	COASTAL
08GA071	ELAHO RIVER NEAR THE MOUTH	1200	34.6	105.0	52.5	6	COASTAL
08GE002	KLINAKLINI RIVER EAST CHANNEL (MAIN) NEAR THE MOUTH	5780	76.0	299.9	149.9	12	COASTAL
08CG001	ISKUT RIVER BELOW JOHNSON RIVER	9500	97.5	465.0	232.5	33	COASTAL
08DB001	NASS RIVER ABOVE SHUMAL CREEK	18400	135.6	806.1	403.1	18	COASTAL
08CE001	STIKINE RIVER AT TELEGRAPH CREEK	29000	170.3	421.3	210.6	39	COASTAL
08EF001	SKEENA RIVER AT USK	42300	205.7	911.6	455.8	34	COASTAL
08NJ026	DUHAMEL CREEK ABOVE DIVERSIONS	52.9	7.3	1.5	0.8	32	INTERIOR
08NG077	ST. MARY RIVER BELOW MORRIS CREEK	208	14.4	7.1	3.6	29	INTERIOR
08NF001	KOOTENAY RIVER AT KOOTENAY CROSSING	416	20.4	4.9	2.4	36	INTERIOR
08NG002	BULL RIVER NEAR WARDNER	1520	39.0	32.5	16.3	40	INTERIOR
08NN026	KETTLE RIVER NEAR WESTBRIDGE	2140	46.3	28.0	14	26	INTERIOR
08NL038	SIMILKAMEEN RIVER NEAR HEDLEY	5580	74.7	48.6	24.3	30	INTERIOR
08NG065	KOOTENAY RIVER AT FORT STEELE	11500	107.2	172.5	86.2	62	INTERIOR
08LF051	THOMPSON RIVER NEAR SPENCES BRIDGE	55400	235.4	778.1	389	79	INTERIOR
08MC018	FRASER RIVER NEAR MARGUERITE	114000	337.6	1456.9	728.5	78	INTERIOR
08MF005	FRASER RIVER AT HOPE	217000	465.8	2720.4	1360.2	100	INTERIOR

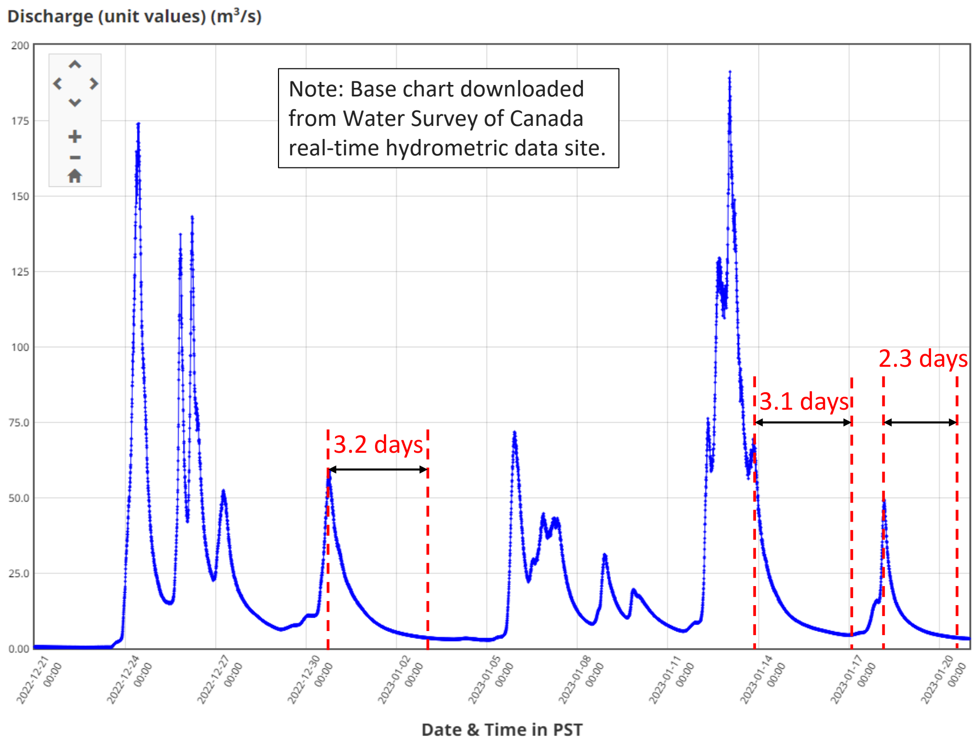

(a) TOFINO CREEK NEAR THE MOUTH (08HB086): $T_0 = 2.3$ to 3.2 days for Dec. 21, 2022 – Jan. 20, 2023

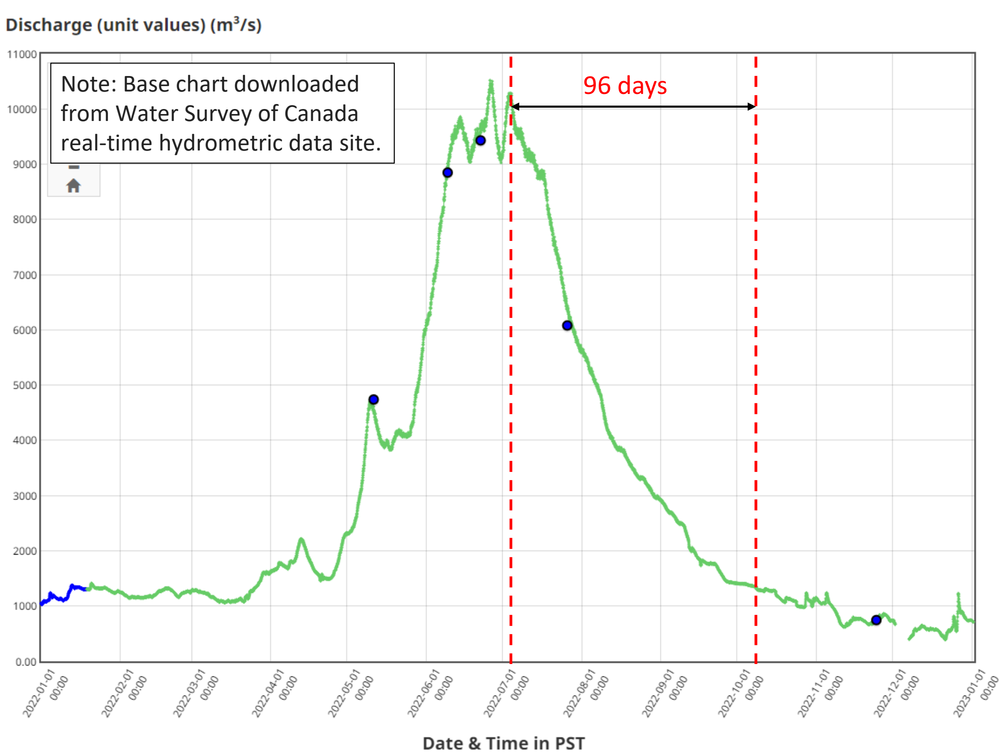

(b) FRASER RIVER AT HOPE (08MF005): $T_0 = 96$ days for 2022

Figure 1. Two extreme examples of T_0 for BC watersheds.

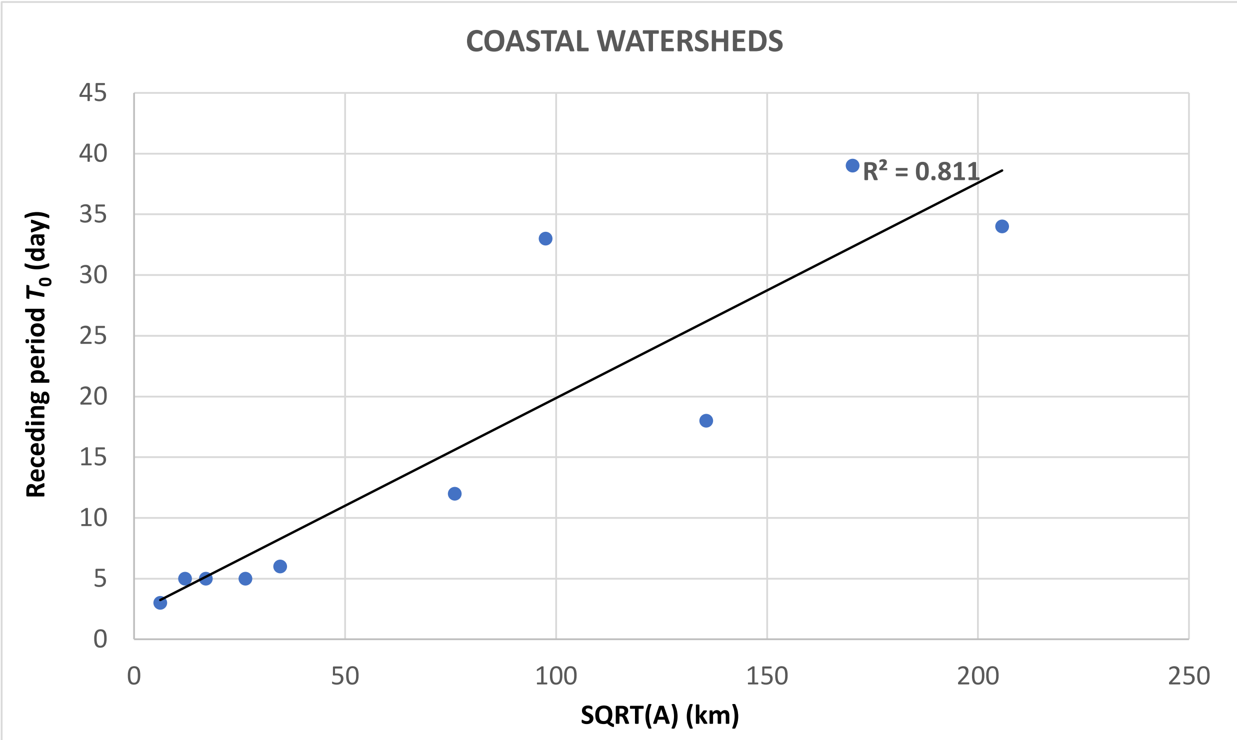

(a) 10 coastal watersheds

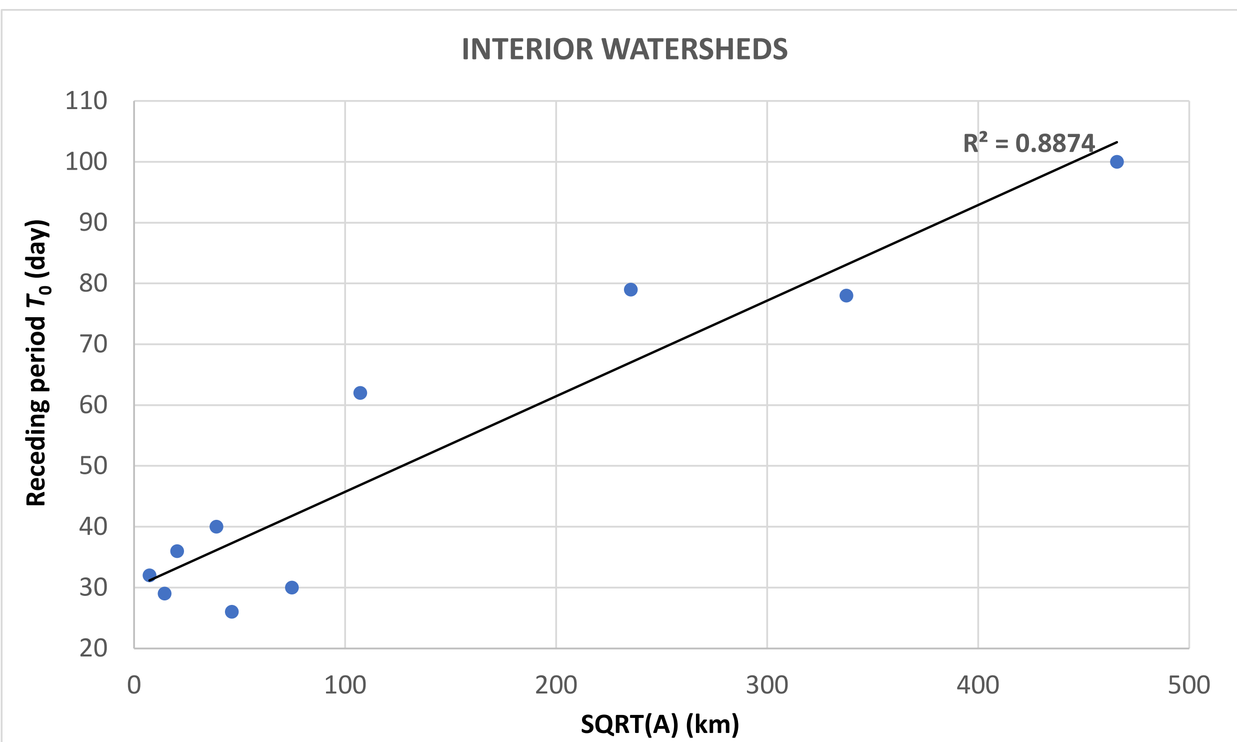

(b) 10 interior watersheds

Figure 2. Correlations between average receding period $\overline{T_0}$ and square root of watershed area.

3. Obstacles faced by low flow simulation with hydrological methods

From the above section, it clear that the magnitude of low flow is very small and sometimes close to zero. From the perspective of flow measurements, the low flow (discharge and water level) is sometimes so trivial or close to zero that it is negligible. The low flow discharge, which is also referred to as baseflow, is bottom parts of the high flow or flood hydrograph. Comparing with the high flow or flood, the baseflow is so small that sometimes it is only about the magnitudes of the measurement errors or forecast errors of any hydrological model. This is the first obstacle of the low flow simulation with hydrological methods.

There are mainly two categories of hydrological models, conceptual/lumped-sum models and physically based distributed models. For most conceptual/lumped-sum hydrological models, the baseflow is a preset constant, and the UBCWM (Quick and Pipes, 1977) is an example of these models. Therefore, this kind of hydrological models have no mechanism to simulate the changing low flow when it falls below the level of the baseflow. This is the second obstacle of low flow simulation with hydrological methods.

For physically based distributed hydrological models, the baseflow in a stream is mainly from the release of the groundwater, except the low flow in the downstream reach of a lake or reservoir, which is mainly from the release of the lake or reservoir. The Large-scale, Unified, and Optimization Model (LUOM) (Luo, 2007) is one example of this model. Practically, groundwater simulation, especially for large-scale watersheds, are faced with two critical difficulties, (1) lack of detail distributed aquifer parameters, and (2) severe deficiency of wells for groundwater observation (Luo, 2000 a). This is particularly true for BC that has a super large area (947,900 km^2), which is the total size of France, Italy, Belgium, and the Netherlands. Nevertheless, BC has only 340 observation wells as part of the Provincial Groundwater Observation Well Network and 1,286 mapped aquifers (45,460 km^2) to cover the entire province in 2023. Figure 3 is a snapshot of BC Groundwater Wells and Aquifers website (BC Gov., 2023 b), which shows the sparsity of observation wells (dark brown dots) and mapped aquifers (brown lines and filled patches). Furthermore, the hydraulic connection between streams and the aquifers which many these wells reside in are unknown, making groundwater-surface water relationships difficult to quantify. This sparse observation wells and mapped aquifers making accurate simulation of groundwater movements and releases to streams in most areas of BC almost impossible. Therefore, it is in turn almost impossible to accurately simulate low flows with distributed hydrological models in most parts of the province. Summarily, the third obstacle of low flow simulation with hydrological methods is the severe insufficiency of groundwater and aquifer data.

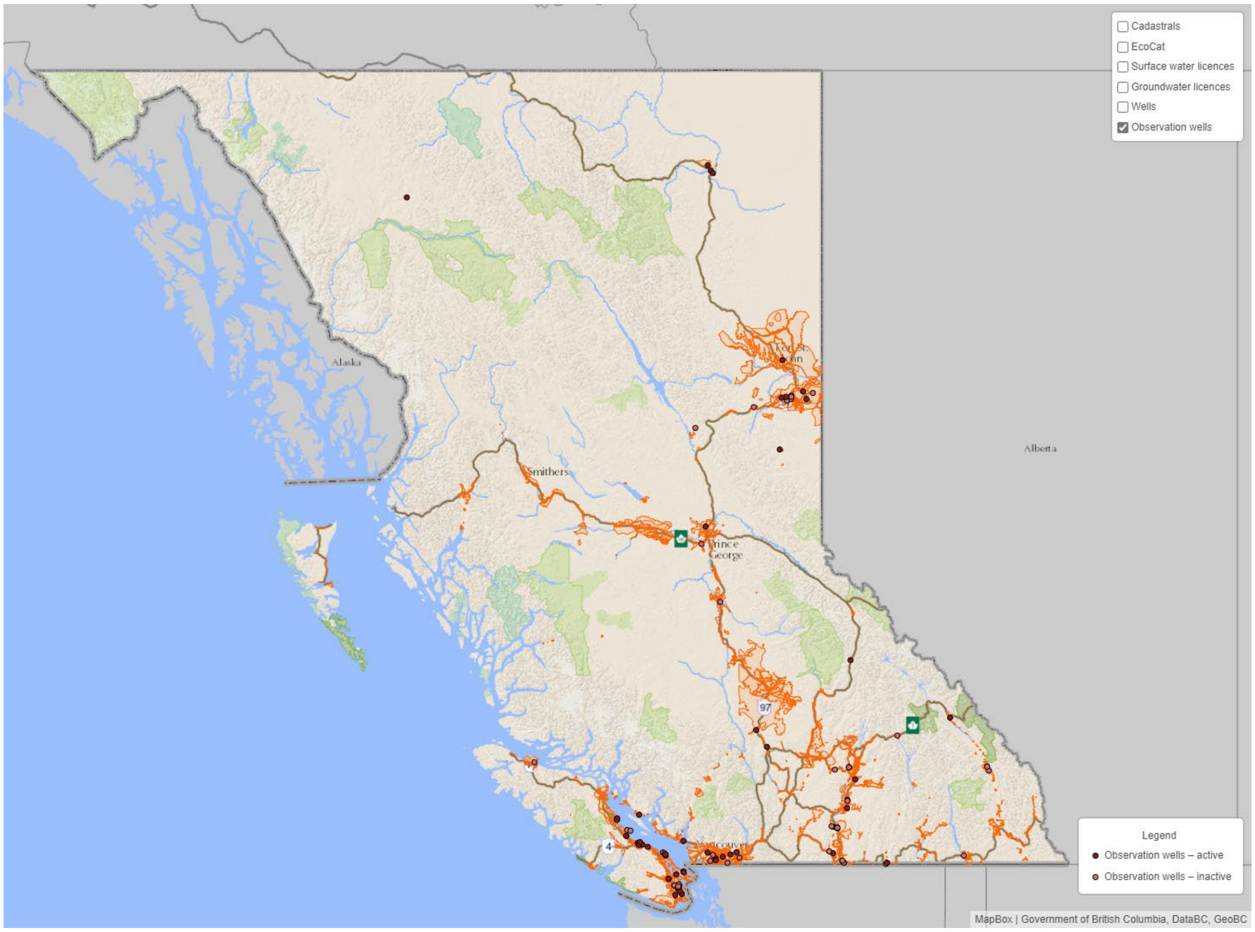

Figure 3. Snapshot of BC Groundwater Wells and Aquifers website showing sparsity of observation wells (dark brown dots) and mapped aquifers (brown lines and filled patches).

4. Fundamental assumption for mathematical methods for low flow forecasting

In order to avoid the obstacles faced by hydrological methods in low flow simulation, it is inevitable to turn to an alternative, empirical or mathematical methods. In Chapter 11 of the Manual on Low flow Estimation and Prediction (WMO, 2008), the recession analysis is classified as the commonly used non-hydrological method for short-term low flow forecasting models, which provide forecasts of low flow in the absence of rainfall between 1 and 20 days.

It sounds like that the recession analysis is a pure mathematical treatment of the flow data without any hydrological process. However, the streamflow is the combined effect of meteorological factors such as rainfall, snowmelt, and evapotranspiration, and watershed physical factors (geological and geomorphological factors) such as the watershed area and the aquifer storage and hydraulic conductivity. For example, the streamflow rises when there is rainfall and/or snowmelt input, and the streamflow recedes acceleratingly when the evapotranspiration rate increases in the watershed; the streamflow recedes faster in a smaller watershed with less groundwater storage than in a larger watershed with more groundwater storage (see Figure 1 in Section 2). This means that the flow data actually includes meteorological signals and watershed physical factors. Therefore, it is possible to accurately simulate the streamflow with flow data input only during the low flow period, employing an appropriate empirical or mathematical equation, and assuming

1) **The sum of the water release rate from the watershed liquid water storage plus the net meteorological liquid water input rate to the streamflow is a function of time and parameters. Equation (4) can be re-written as**

$$Q = \Phi + \Psi = f(p_i, t) \tag{11}$$

in which $p_i, i = 1\ to\ N$ are parameters of the function.

2) **The function parameters p_i remain constant for a certain period.**

This is the fundamental assumption for the ELF Model. When the low flow conditions meet this assumption, the forecast is accurate, otherwise, the forecast is inaccurate.

It must be emphasised that this assumption does not prescribe that net meteorological water input rate must be equal to 0. This rate could be positive, 0 or negative. For this reason, the ELF Model can be run all year round and sometimes can even accurately forecast minor rises in the low flow, especially for lake water levels.

It must be also pointed out that the function parameters are constant only for a certain period but not all-time constants. This gives the ELF Model flexibility to adjust it forecasts based on the most recently available flow data.

5. Basic equations of mathematical method for low flow simulation and extended characteristic of low flow

It was found that the basic behaviour of the daily mean flow ($Q(t)$) on the falling limb of the hydrograph is mainly characterized by the following exponential recession equation (Reed and Warne, 1985; WMO, 2008)

$$Q(t) = Q_0 e^{-\alpha t} \tag{12}$$

in which t is time, α is a positive constant, e is the base of the natural logarithm, and Q_0 is the initial discharge when $t = 0$.

Equation (12) is a time function with three parameters, Q_0, e, and α, which are all constants, and therefore fulfills the fundamental assumption of the ELF Model given in the above section.

Conducting logarithmic calculation on both sides of Equation (12), simplifying notation $Q(t)$ to Q, and after some rearrangements, Equation (12) can be rewritten as

$$ln(Q) = -\alpha t + ln(Q_0)$$

(13)

Carrying out derivative calculation on both side of Equation (13) with respect to time t

$$\frac{d}{dt}[ln(Q)] = \frac{d}{dt}[-\alpha t + ln(Q_0)]$$

(14)

$$\frac{1}{Q}\frac{dQ}{dt} = -\alpha$$

(15)

Or

$$\frac{dQ}{dt} = -\alpha Q$$

(16)

As both α and Q are positive, the physical meaning of Equation (16) is that the streamflow is decreasing. This is the first characteristic of low flow summarized in Section 2.

Carrying out derivative calculation on both sides of Equation (16) with respect to time t and substituting Equation (16) in it, the second-order derivative of Q of time is given by

$$\frac{d^2Q}{dt^2} = \alpha^2 Q$$

(17)

The physical meaning of Equation (17) is that the slope of the change of streamflow (dQ/dt) is increasing. For the change of streamflow that is always negative or $dQ/dt \leq 0$, "increasing" actually means that the decreasing rate of the streamflow becomes smaller and smaller, or the decreasing trend becomes slower and slower with time. This is an extended characteristic of low flow.

Summarily, the first characteristic of low flow is extended as the following,

a. <u>The streamflow is decreasing, and the decreasing rate of the streamflow becomes smaller and smaller with time.</u>

The falling limb of streamflow data used in this study always shows this characteristic of low flow, and the hydrographs shown in Figure 1 in Section 2 are two examples.

In this study, quite a number of flow stations have water level data only, and for those stations with both discharge and water level data, it is anticipated that the model can forecast both discharges and water levels. In order to use the water level data to produce low flow forecasts, it is necessary to prove that the water level h in the low flow regime also has the same characteristics shown in Equations (16) and (17).

During the low flow period, the flow rate (q) along the groundwater releasing cross section A_G can be written in the following partial differential form of the Darcy's Law (Luo, 2000 b)

$$q = K\frac{\partial h}{\partial x}$$

(18)

in which K is the hydraulic conductivity of the aquifer and assumed constant along the riverside during the low flow period, h is the water level of the groundwater and the water level of the streamflow, and x is the distance from the stream which is perpendicular to the stream. Assuming $\partial h/\partial x = S_0$, which is the slope of the bedrock and is a constant during the low flow period, and $A_G = Bh$, B is the width of the groundwater releasing cross section, the discharge from the groundwater release can be written as

$$Q = qA_G = (KS_0B)h = \beta h$$

(19)

in which β is a constant.

Substituting Equation (19) into Equations (16) and (17), the following equations can be derived

$$\frac{dh}{dt} = -\alpha h$$

(20)

$$\frac{d^2h}{dt^2} = \alpha^2 h$$

(21)

This means that the water level during the low flow period follows the same receding trend as the discharge that can be simulated with Equation (12) by substituting Q with h. Hereinafter, descriptions about "low flow" or "flow" means discharge and water level, and all equations for Q (discharge) are also valid for H (water level), if not explicitly stated.

6. Solving exponential recession equation for overdetermined system

Equation (13) is a linear equation with the following form

$$y = ax + b$$

(22)

noticing that

$$\begin{cases} y = \ ln(Q) \\ x = t \\ a = -\alpha \\ b = \ ln(Q_0) \end{cases}$$

(23)

If there is a series of observations (e.g., 30 days of data), Equation (22) becomes an overdetermined system. Assuming f is a notation of the function for Equation (22)

$$f = y = ax + b$$

(24)

The least squares linear fitting method is adopted to find the theoretical curve for the observed data points of low flow

$$\begin{cases} R^2 = \sum_{i=1}^{n} \left[y_i - f\left(x_i, a_1, a_2, \dots, a_j, \dots, a_m\right) \right]^2 \\ \frac{\partial (R^2)}{\partial a_i} = 0, i = 1 \; to \; n \end{cases}$$

(25)

in which R^2 is the square of the vertical deviations, i is the sequence of the data points, n is the total number of data, j is the sequence of independent parameters a_j, and m is the total number of parameters in the function.

In the case of Equation (24), $m = 2$, $a_1 = a$, and $a_2 = b$. Parameters a and b can be found with

$$\begin{cases} a = \frac{\sum_i^n (x_i y_i) - n\bar{x}\bar{y}}{\sum_i^n x_i^2 - n\bar{x}^2} \\ b = \frac{\bar{y}\sum_i^n x_i^2 - \bar{x}\sum_i^n (x_i y_i)}{\sum_i^n x_i^2 - n\bar{x}^2} \end{cases}$$

(26)

where

$$\begin{cases} \bar{x} = \frac{1}{n}\sum_{i=1}^{n} x_i \\ \bar{y} = \frac{1}{n}\sum_{i=1}^{n} y_i \end{cases}$$

(27)

7. Twelve-step and twelve-scenario scheme for meeting challenges posed by data issues of noises and non-logarithmic flow and for analogues to ensemble forecasts

It is noticed that, in the real world, the actual low flow data always include noises, which are sharp rises and steep falls caused by sudden changes of meteorological conditions, such as changes in the input of rainfall, snowmelt or glacier melt, and increasing evapotranspiration due to high temperatures, and measurement errors in the flow data. This is the so-called “data noise issue” in the low flow simulation. Meanwhile, the low flow data, especially the water level data, may not always follow the trend governed by Equation (12), or the logarithmic low flow time series are not always linear. This is the so-called “non-linear logarithmic flow issue” in the low flow simulation. These issues of data noises and non-linear logarithmic flows in the actual low flow data prevent low flow models using Equations (12) to (27) from producing accurate forecasts.

Figure 4 shows three time series of discharges or water levels for a 60-day period, (a) is a time series with significant data noises, (b) and (c) are time series of non-linear logarithmic discharges and water levels, respectively. The red dash lines are the trendlines of the flow data from the first 30 days, which would never give any correct forecast for the flows of the second 30 days due to the data noises issue and the non-linear logarithmic flow issue, let alone an accurate forecast.

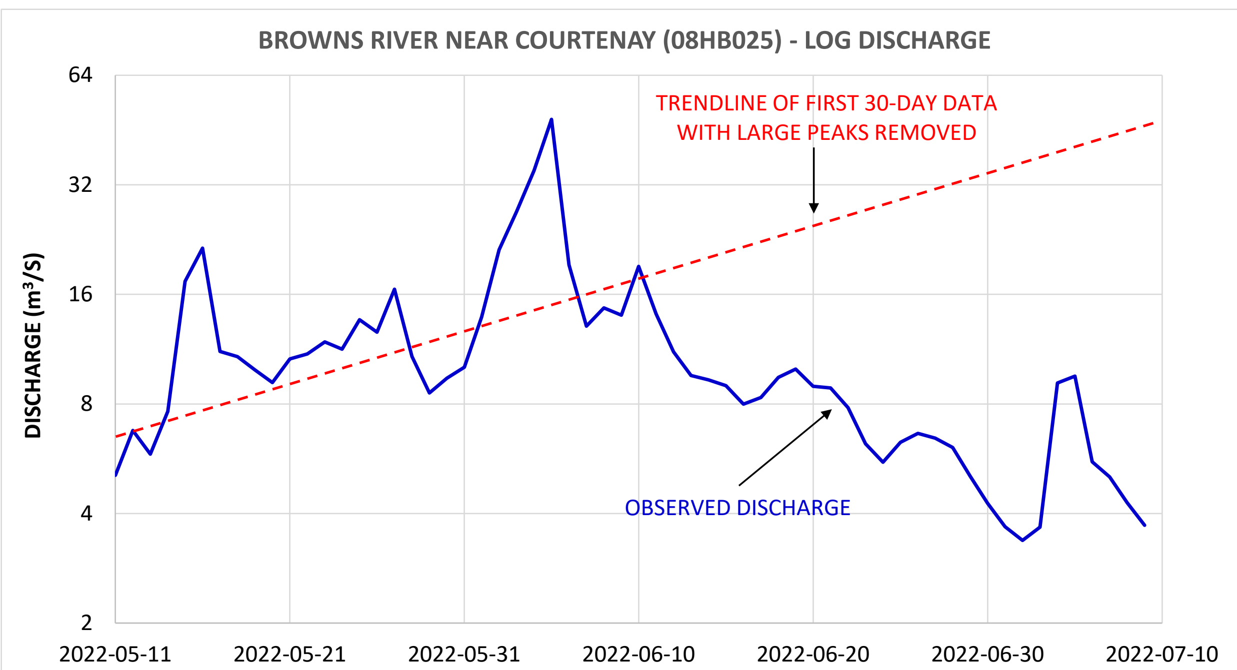

(a) Significant data noises – BROWNS RIVER NEAR COURTENAY (08HB025) (A = 87.9 km^2) (May 11 to July 9, 2022)

Figure 4. Examples of low flow data issues (continued on next page).

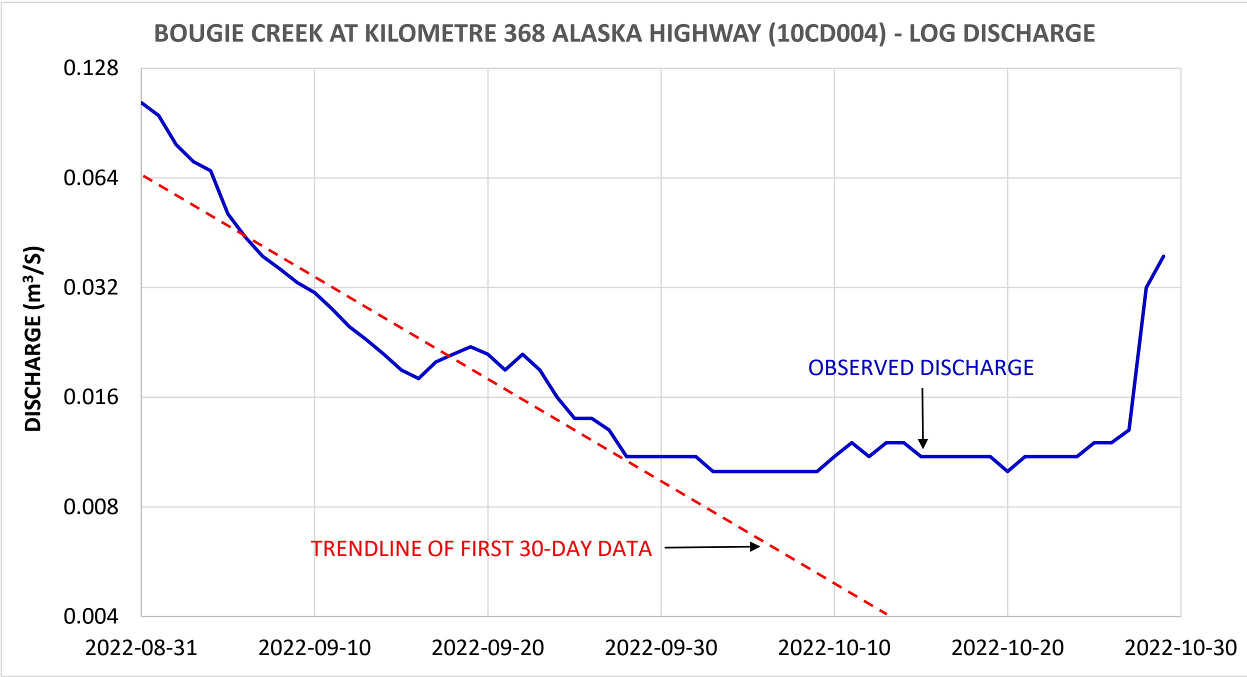

(b) Non-linear logarithmic flow – daily discharge for BOUGIE CREEK AT KILOMETRE 368 ALASKA HIGHWAY (10CD004) (A = 335 km^2) (August 31 to October 29, 2022)

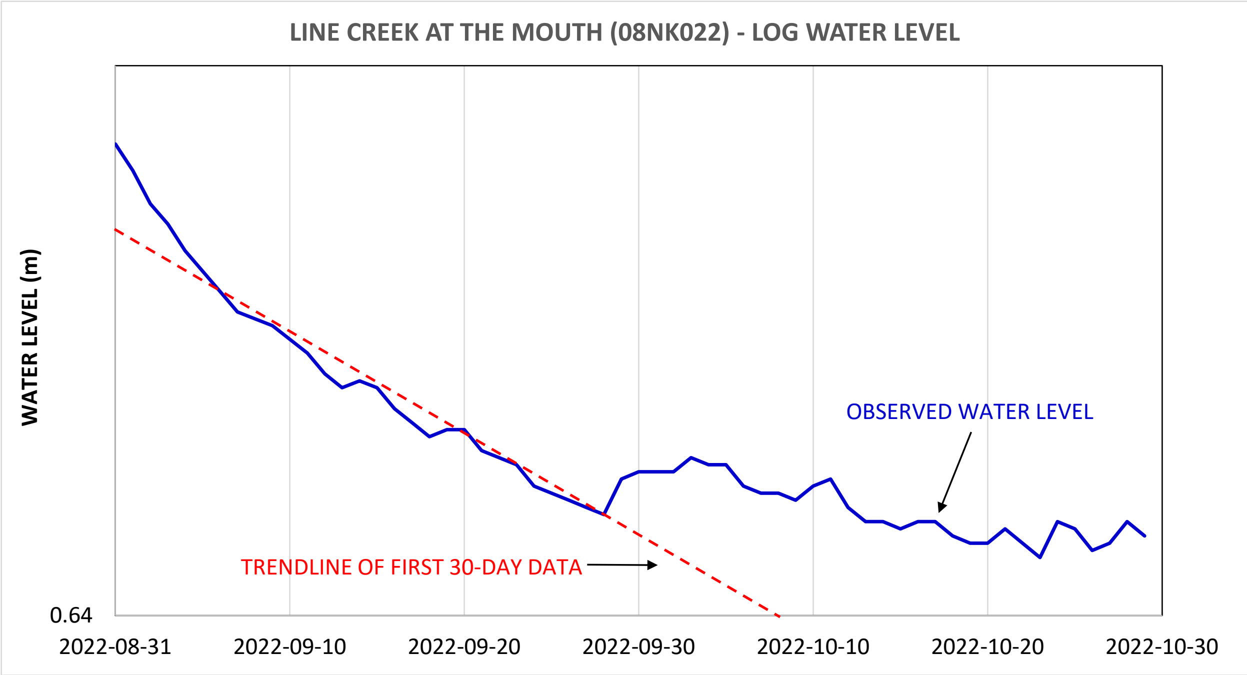

(c) Non-linear logarithmic flow – daily water level for LINE CREEK AT THE MOUTH (08NK022) (A = 138 km^2) (August 31 to October 29, 2022)

Figure 4. Examples of low flow data issues (continued).

To filter out flow data noises, a baseflow separation method was developed in the United Kingdom (Gustard, 1983; Gustard et al., 1992). In this method, the flow data is split into five-day non-overlapping consecutive periods, for which the minimums are found. The turning points are searched from the minimums, and then the baseflow hydrograph is obtained by connecting the turning points. Checking with Table 1 in Section 2, it is obvious that the above five-day baseflow separation method works well for the coastal watersheds that have an area from 100 to 1000 km^2, which have a receding period about 5 days. However, this method does not make sense for those watersheds with a receding period short or longer than 5 days, especially for the interior watersheds, in which the receding period is much longer than 5 days (26 days and longer, see Table 1).

In order to meet the challenges posed by the flow data issues of data noises and non-linear logarithmic flows, a numerical scheme, the so-called "twelve-step and twelve-scenario scheme" based Equations (12) to (27), is developed in this study. The scheme not only is more appropriate for BC watersheds with respect to filtering out data noises, but also produces forecast maximums and minimums which are analogues to ensemble forecasts. In the ELF Model, a time series of 30-day observed flows is used to produce a 30-day forecast using a time step of one day for the immediate 30 days. The scheme is given in detail below.

Step 1. Preparing the input data – the observed daily discharge (Q_i) and water level (H_i) so that

$$\begin{cases} Q_i = Q_{obsi} > 0 \\ H_i = H_{obsi} - H_{min} > 0 \end{cases} \tag{28}$$

where Q_{obsi} is the observed daily average discharge on day i, eliminating 0 and negative values, H_{obsi} is the observed daily average water level on day i, and H_{min} is the historical minimum water level. Water levels for some flow stations in BC have negative datum and may be negative. The treatment in Equations (28) is necessary to ensure that the values of observed discharges and water levels are positive so that logarithmic calculations for these data are valid.

Step 2. Calculating the logarithms for observed discharges and water levels to the base of 10, $\log Q_i$ (and $\log H_i$). In this study, the logarithm with a base of 10 rather than the natural logarithm is adopted because some of the discharges are very large, as large as 10,000 m^3/s in the summer for the FRASER RIVER AT HOPE (08MF005), and the ELF Model is updated for all the year round. It can be proved that Equations (16) and (17) are still true for the logarithms of discharges and water levels with a base of 10.

Step 3. Calculating 5-day moving averages of $\log Q$ (and $\log H$) day by day for the observed discharges and water levels (equations for the water level have the exact same format)

$$\left(\overline{\log Q}\right)_j = \frac{1}{5}\sum_{i=d}^{d+4} \log Q_i \tag{29}$$

in which j is the time sequence of the 5-day moving average, and d is a day of the observed daily time series. And if J is the total data points of $\left(\overline{\log Q}\right)_j$ for a time series of observed discharges or water levels for a total days of D, $J = D - 4$. In this study, $D = 30$, and thus $J = 26$.

Step 4. Calculating the increment of the 5-day moving average of $\left(\overline{\log Q}\right)_j$

$$\left(\Delta\,\overline{\log Q}\right)_l = \left(\overline{\log Q}\right)_{j+1} - \left(\overline{\log Q}\right)_j = \frac{1}{5}(\log Q_{i+5} - \log Q_i) \tag{30}$$

in which l is the time sequence of $\Delta\,\overline{\log Q}$. If L is the total number of $\left(\Delta\,\overline{\log Q}\right)_l$, $L = J - 1 = 25$ in this study.

$\Delta\,\overline{\log Q}$ is the difference form of the time derivative of $\overline{\log Q}$. Carrying out derivative calculation on both sides of Equation (22), the following equation can be derived if $\Delta\mathrm{t} = 1$ (day)

$$\Delta\,\overline{\log Q} \approx d\left(\overline{\log Q}\right)\Delta\mathrm{t} \approx dy = a \tag{31}$$

Equation (31) means that $\Delta\,\overline{\log Q}$ is a constant.

However, as pointed out at the beginning of this section, the flow data may have the non-linear logarithmic flow issue. This means that the observed daily time series of discharges or water levels may not strictly fulfill Equations (12) and (22). In order to meet the challenge posed by the non-linear logarithmic flow issue, it is assumed that the derivative of the averaged logarithmic flow (discharge or water level) is also a linear line rather than a constant,

$$\Delta\,\overline{\log Q} \approx d\left(\overline{\log Q}\right)\Delta\mathrm{t} \approx dy = ax + b \tag{32}$$

Of course, when the observed data of $\Delta\,\overline{\log Q}$ is fitted in Equation (32) using Equations (26) and (27), Equation (32) will reduce to Equation (31) if it is found that $a = 0$ and b is re-noted as a.

Step 5. Calculating the increment of $\left(\Delta\,\overline{\log Q}\right)_l$

$$\left(\Delta\Delta\,\overline{\log Q}\right)_n = \left(\Delta\,\overline{\log Q}\right)_{l+1} - \left(\Delta\,\overline{\log Q}\right)_l \tag{33}$$

in which n is the time sequence of $\Delta\Delta\,\overline{\log Q}$. If N is the total number of $\Delta\Delta\,\overline{\log Q}$, $N = L - 1 = 24$ in this study.

$\Delta\Delta\,\overline{\log Q}$ is the difference form of the time derivative of $\Delta\,\overline{\log Q}$. If derivative calculation for both sides of Equation (31) is carried out, the following equation can be derived when $\Delta\mathrm{t} = 1$ (day)

$$\Delta\Delta\,\overline{\log Q} \approx d\left(d\left(\overline{\log Q}\right)\right)\Delta\mathrm{t} \approx d(dy) = da = 0 \tag{34}$$

And if derivative calculation for both sides of Equation (32) is carried out, the following equation can be derived when $\Delta t = 1$ (day)

$$\Delta\Delta\,\overline{\log Q} \approx d\left(d\left(\overline{\log Q}\right)\right)\Delta t \approx d(dy) = d(ax+b) = a \tag{35}$$

Equations (34) and (35) together mean that $\Delta\Delta\,\overline{\log Q}$ is a constant, either 0 or non-zero. This is a very important characteristic of low flow for the ELF Model in this study.

Step 6. _Scenario 1_ – Fitting 25 points of $\Delta\,\overline{\log Q}$ in Equation (32) using Equations (26) and (27). Once a and b are determined, the last five data points of $\log Q_i$ for $i = 26$ to 30 is used for bias correction.

$$\begin{cases} \Delta\log Q_{simi} = a(i-5) + b \\ \log Q_{simi} = \log Q_{simi-1} + \Delta\log Q_{simi} \\ \log Q_{sim0} = \log Q_{obs25} \\ Bias = \dfrac{1}{5}\left(\displaystyle\sum_{i=26}^{30} \log Q_{simi} - \sum_{i=26}^{30} \log Q_{obsi}\right) \end{cases} \tag{36}$$

in which $\log Q_{sim}$ is the model simulated logarithmic flow (discharge or water level), $\Delta\log Q_{sim}$ is the simulated increment of $\log Q_{sim}$, $\log Q_{obs}$ is observed logarithmic flow, and $Bias$ is the deviation between the means of observation and simulation of the last 5 days, which is the bias correction.

After the bias correction is calculated, the model forecast Q_j ($j = 1$ to 30) (discharge and water level) for the next 30 days can be estimated with the following equations

$$\begin{cases} \Delta\log Q_{simj} = a(j+30) + b \\ LQ_j = \log Q_{simj} = \log Q_{simj-1} + \Delta\log Q_{simj} \\ \log Q_{sim0} = \log Q_{obs30} \\ Q_j = 10^{(LQ_j - Bias)} \end{cases} \tag{37}$$

In order to reduce unrealistic forecasts, $\Delta\log Q_{sim}$ in both Equations (36) and (37) is subject to restrictions as given in the following equations

$$\begin{cases} \Delta\log Q_{simj} \le 0.1\,\Delta\log Q_{sim0j}\,, \quad \text{if } \Delta\log Q_{sim0j} > 0 \\ \dfrac{\Delta\log Q_{simj}}{\Delta\log Q_{simj-1}} \le 1.01, \text{if } \Delta\log Q_{simj}\,, \Delta\log Q_{simj-1} < 0 \end{cases} \tag{38}$$

in which $\Delta\log Q_{sim0j}$ is the original estimation with Equation (37). Equations (38) mean that the final forecast rate of rise in the logarithmic flow only takes 10% of the simulated rate of rise into account, and the forecast drops in the logarithmic flow must not be accelerated by a rate greater than 1%.

It was found later (as of July 17, 2023, when this report was being compiled) that the original estimate of $\Delta\log Q_{sim}$ is able to simulate rises for water levels accurately for some of the water-level-only stations. Therefore, the first half of Equations (38) is modified as below

$$\begin{cases} \frac{\Delta \log Q_{simj}}{\Delta \log Q_{simj-1}} \leq 1, \text{ if } \Delta \log Q_{simj}, \Delta \log Q_{simj-1} > 0 \\ \frac{\Delta \log Q_{simj}}{\Delta \log Q_{simj-1}} \leq 1.01, \text{if } \Delta \log Q_{simj}, \Delta \log Q_{simj-1} < 0 \end{cases}$$

(39)

The modification in Equations (38), or the first equation of Equations (39) means that the forecast rises for the logarithmic flow must not be accelerated.

Step 7. Calculating the mean of $\left(\Delta\Delta\,\overline{\log Q}\right)_n$ $(n = 1 \text{ to } 24)$ and the deviation of each data point from the mean, ranking $\left(\Delta\Delta\,\overline{\log Q}\right)_n$ by the deviation in the order from the smallest to the largest. Equations (33) and (34) indicate that $\left(\Delta\Delta\,\overline{\log Q}\right)_n$ should be a 0 or a non-zero constant. However, the actual data may not strictly fulfill these equations. The ranks will be used by the next step.

Step 8. _Scenario 2 to 8_ – Eliminating data points of $\left(\Delta\,\overline{\log Q}\right)_l$ $(l = 2 \text{ to } 25)$ with the 2, 4, 6, 8, 10, 12, and 14 largest deviations of $\left(\Delta\Delta\,\overline{\log Q}\right)_n$ $(n = 1 \text{ to } 24)$ from the mean found in Step 7, and fitting the rest of data points of $\Delta\,\overline{\log Q}$ excluding the first data point (number of data points for each scenario is 22, 20, 18, 16, 14, 12, and 10, respectively) in Equation (32) using Equations (26) and (27). The first data point of $\Delta\,\overline{\log Q}$ is not used because $\left(\Delta\Delta\,\overline{\log Q}\right)_n$ has one data point fewer than $\Delta\,\overline{\log Q}$. Once a and b are found, the model forecast Q_j $(j = 1 \text{ to } 30)$ (discharge and water level) for the next 30 days can be estimated with Equations (36) to (39) given in Step 6.

Step 9. _Scenario 9_ – Fitting the 10 data points of $\left(\Delta\,\overline{\log Q}\right)_l$ in the last 15 days $(l = 11 \text{ to } 25)$, which have the minimum deviations of $\left(\Delta\Delta\,\overline{\log Q}\right)_n$ $(n = 10 \text{ to } 24)$ from the mean, in Equation (31). Or, fitting the same data in Equation (32) with $a = 0$, Equation (26) reduces to

$$\begin{cases} a = 0 \\ b = \bar{y} \end{cases}$$

(40)

The model forecast Q_j $(j = 1 \text{ to } 30)$ (discharge and water level) for the next 30 days also can be estimated with Equations (36) to (39) given in Step 6.

Step 10. _Scenario 10 to 12_ – Fitting the last 10, 5, and 2 data points of $\left(\Delta\,\overline{\log Q}\right)_l$ $(l_{10} = 16 \text{ to } 25;$ $l_5 = 21 \text{ to } 25;$ $l_2 = 24 \text{ to } 25)$ in Equation (31), or Equation (32) with Equation (40), to estimate a and b.

Because these three scenarios use fewer data points from the last days and no data points with noises are excluded, b estimated with Equation (40) could be too large. Therefore, the largest b of these three scenarios is cut to its half, the second largest b is restricted to a value which is not greater than 1.1 times of the modified largest b, and the smallest b must not be larger than 1.1 times of the modified second largest b. These three scenarios ensure that the ELF Model captures the latest trends of the observed flow to increase the chances of accurate forecasts.

Step 11. Finding the forecast maximum and minimum from the 12 scenarios for each day of the 30-day forecasting period, and the forecast average is the average of the forecast maximum and minimum.

Step 12. Restricting the forecast maximum and minimum and recalculating the forecast average with the restricted forecast maximum and minimum. When there was a recent rainfall/melt event, the forecast rise and/or drop may be significantly affected by the event and may not be realistic. In order to reduce the forecast errors, the forecast maximum and minimum are restricted to certain ranges. In this study, a recent rainfall/melt event is defined as the case when the maximum observed daily flow in the latest 15 days is 3 times of the minimum observed daily flow in the past 30 days. "Flow" may also be water level H_i defined by Equation (28) in Step 1. In this case, the forecast maximum must not be larger than the maximum observed daily flow in the latest 15 days if the forecast flow is rising, and the forecast minimum must not be smaller than 20% of the observed minimum daily flow in the past 30 days if the forecast flow is dropping.

With this "twelve-step and twelve-scenario scheme," the ELF Model is able to accurately forecast the flows for the second 30 days by using the observed flows from the first 30 days in the examples of flow time series with the data noise issue and non-linear logarithmic flow issue shown in Figure 4 at the beginning of this section. Figure 5 shows the ELF Model operational outputs of comparisons of the model forecasts and the observed hydrographs.

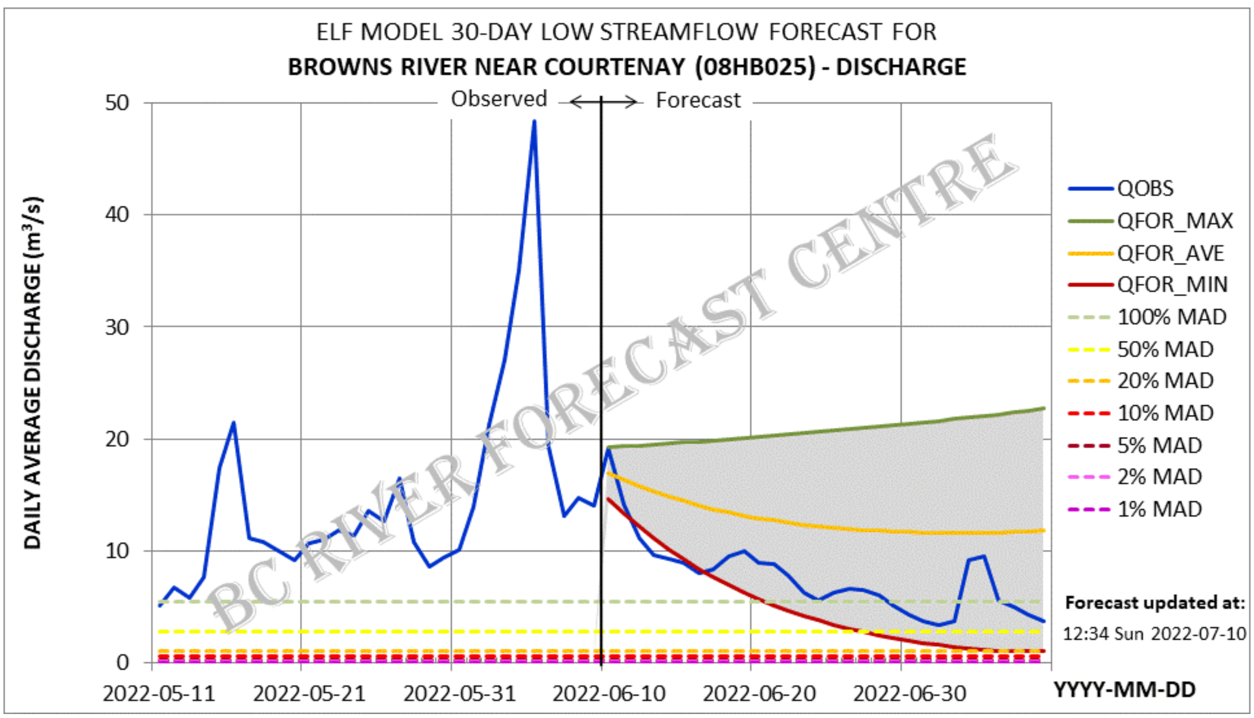

(a) Significant data noises – BROWNS RIVER NEAR COURTENAY (08HB025) (forecast period: June 10 to July 9, 2022)

Figure 5. Examples of ELF Model accurate forecasts for observed flows with data issues (continued on next page).

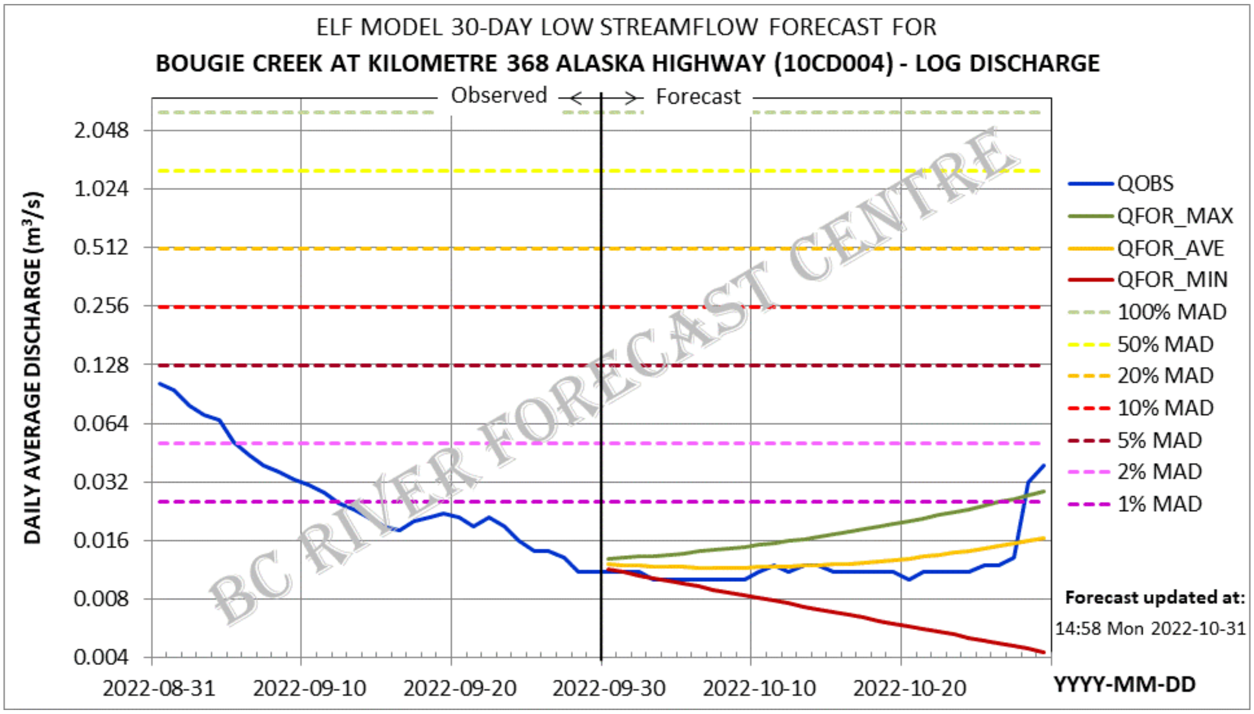

(b) Non-linear logarithmic flow – daily discharge for BOUGIE CREEK AT KILOMETRE 368 ALASKA HIGHWAY (10CD004) (A = 335 km^2) (forecast period: September 30 to October 29, 2022)

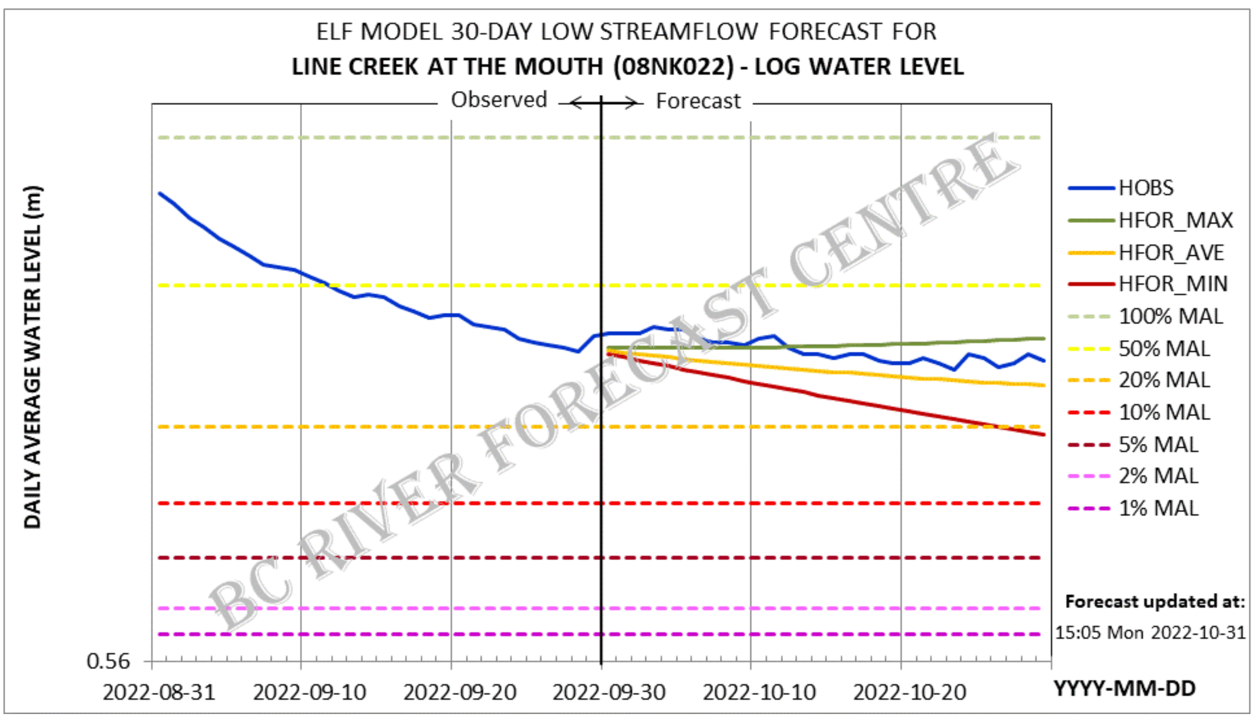

(c) Non-linear logarithmic flow – daily water level for LINE CREEK AT THE MOUTH (08NK022) (A = 138 km^2) (forecast period: September 30 to October 29, 2022)

Figure 5. Examples of ELF Model accurate forecasts observed flows with data issues (continued).

8. Products of ELF Model

The ELF Model generates a series of products in one run as follows,

(1) a GIS map with color coded markers. The color schemes are related to the forecast minimum, average, or maximum discharges comparing with the mean annual discharge (MAD) for stations which have both discharge and water level data, or the forecast minimum, average, or maximum water levels comparing with the mean annual water levels (MAL) for stations which have only water level data. Figure 6 is a Maphub GIS map of the ELF Model forecast updated at 10:44 am August 8, 2023, (a) is the map with the color-coded markers for the forecast minimum (default), and (b) shows the statistics of use of the map layer in the past 12 month (August 9, 2022 to August 9, 2023), showing a total visits of 19,133. The maximum number of daily accesses is 573 on July 12, 2023, and the largest number of monthly access occurs in July of the year (5,495 visits, more than 1/4 of the total annual access).

(2) interactive charts of forecast hydrographs of discharges and/or water levels. The vertical (y) axes of these charts can be toggled between linear and logarithmic scales. Very small discharges or water levels are easier to read in the charts with a logarithmic y axis. In an interactive chart, the exact values of data points in the hydrographs can be displayed when the mouse hovers over the data points. Figure 7 (a) to (d) are examples of interactive charts of discharges and water levels with linear and logarithmic y axes.

(3) static charts of forecast hydrographs of discharges and/or water levels. Static charts are convenient for presentation purposes. Figure 8 (a) to (d) are examples of static charts of discharges and water levels with linear and logarithmic y axes.

(4) forecast verifications for the previous month and a similar period of the previous year. After the ELF Model has finished generating forecasts for the current day, it uses 30 days of observed flow data starting from the same day in the previous month as the current day or the closest day in the previous month to the current day to generate a 30-day "forecast" for each station and plots the "forecast" and the observed hydrographs on the same chart. A link for comparison of the forecast and the observed flow for a similar period in the previous year are also provided on the website. These comparisons of previous forecasts and observed flows provide a visual verification of the model forecast accuracy for a station. Figures 9 and 10 (a) to (b) are examples of static charts of these comparisons.

(5) text (csv) files of the daily forecast. The ELF Model also generates a text (csv) file for each station which includes the forecast flow (discharge and/or water level) for the next 30 days and the observed flow for the immediate recent 30 days. If the forecast is for verification, the text (csv) file also has additional 30 days of observed flow for the forecasting period.

As of July 27, 2023, the ELF Model forecast webpages also provide links to the statistical bar charts of the ELF Model historical forecast accuracy so that users may have a better idea about the model forecast accuracy. This will be discussed in detail in Section 9.

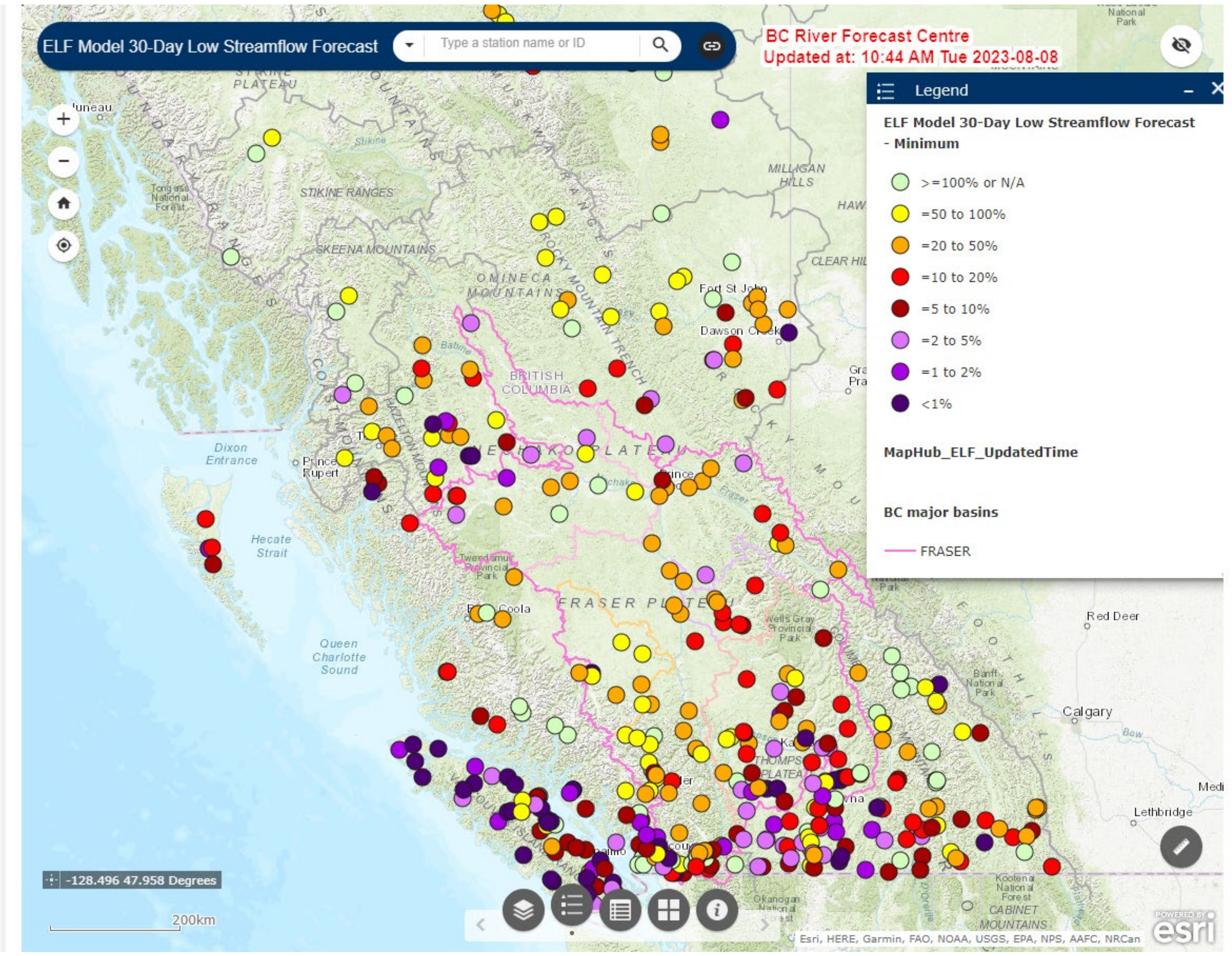

(a) Maphub GIS map of ELF Model (http://bcrfc.env.gov.bc.ca/lowflow/map_elf.html)

(b) Statistics of use of the map layer in past 12 months

Figure 6. A Maphub GIS map of ELF Model forecast updated on Augest 8, 2023

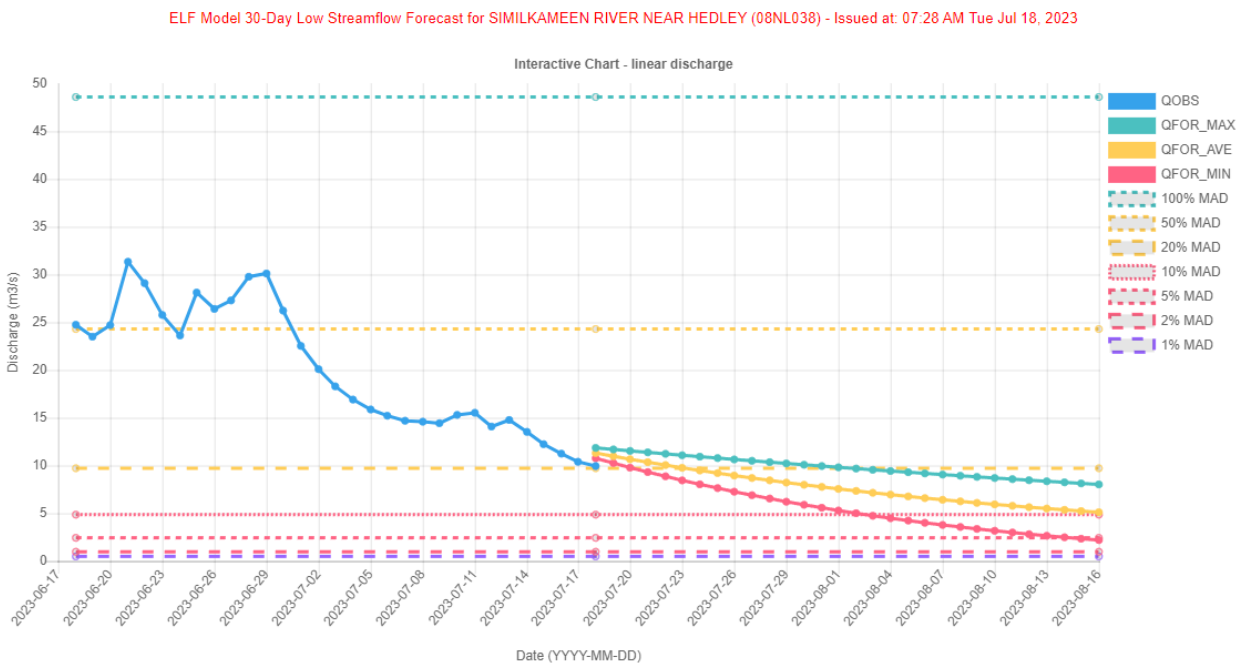

(a) Linear discharge

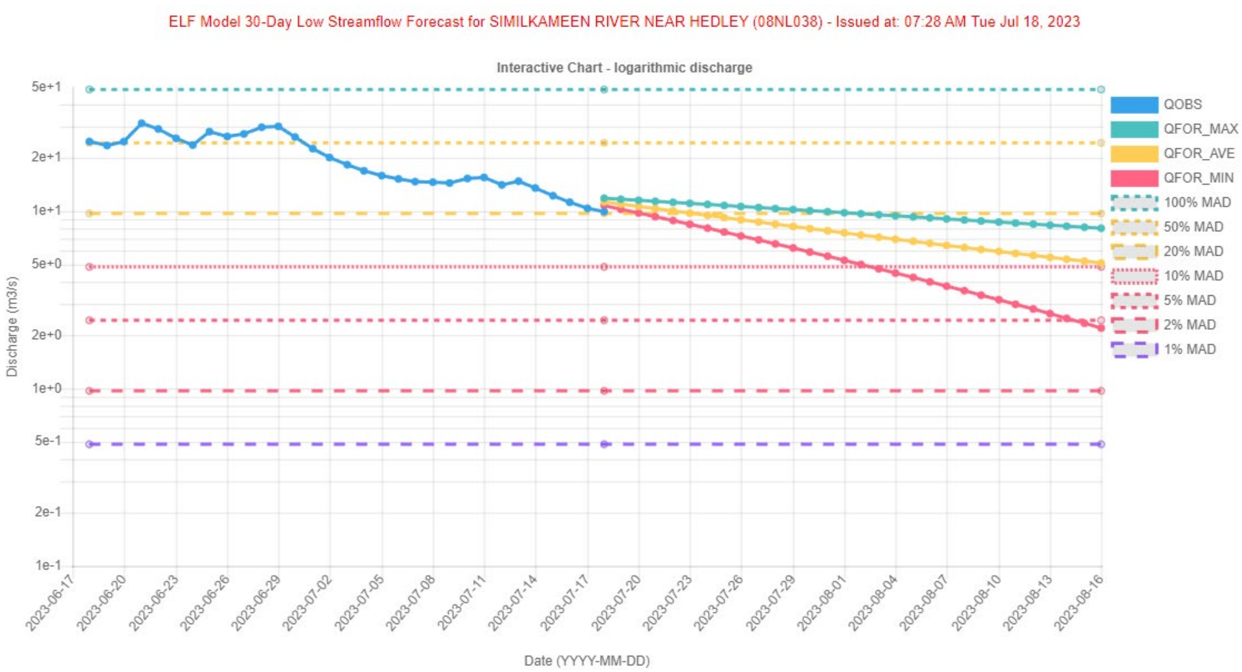

(b) Logarithmic discharge

Figure 7. Interactive charts of ELF Model forecast – SIMILKAMEEN RIVER NEAR HEDLEY (08NL038) (continued on next page.)

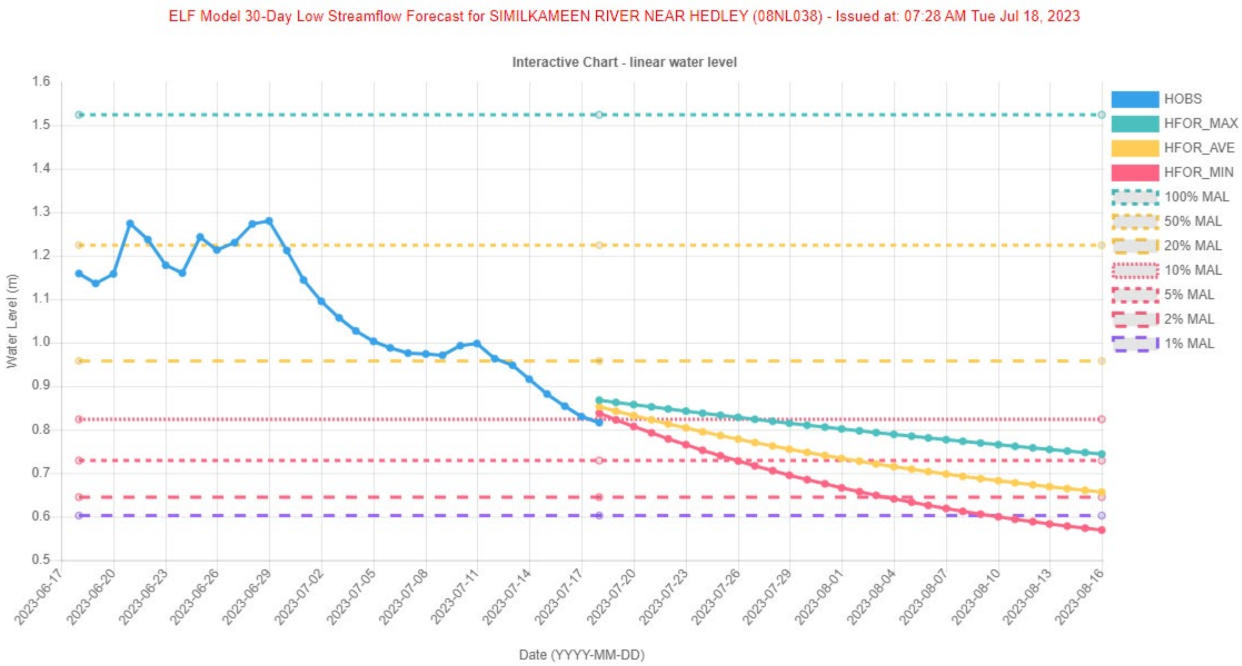

(c) Linear water level

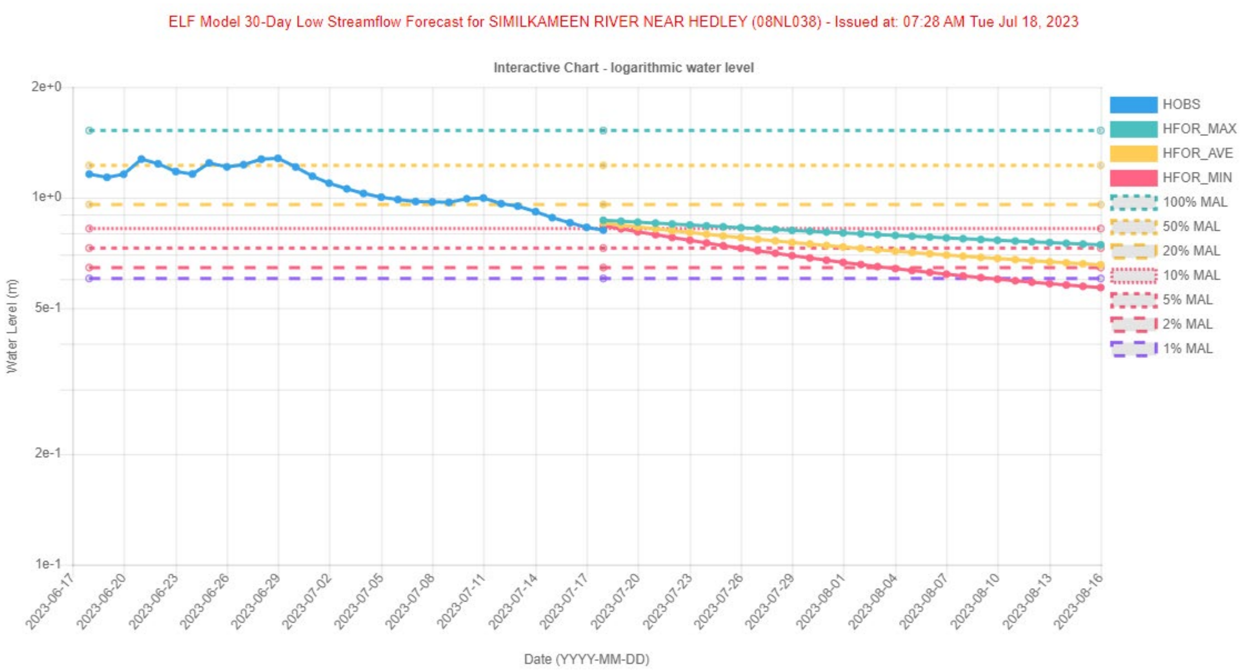

(d) Logarithmic water level

Figure 7. Interactive charts of ELF Model forecast – SIMILKAMEEN RIVER NEAR HEDLEY (08NL038) (continued.)

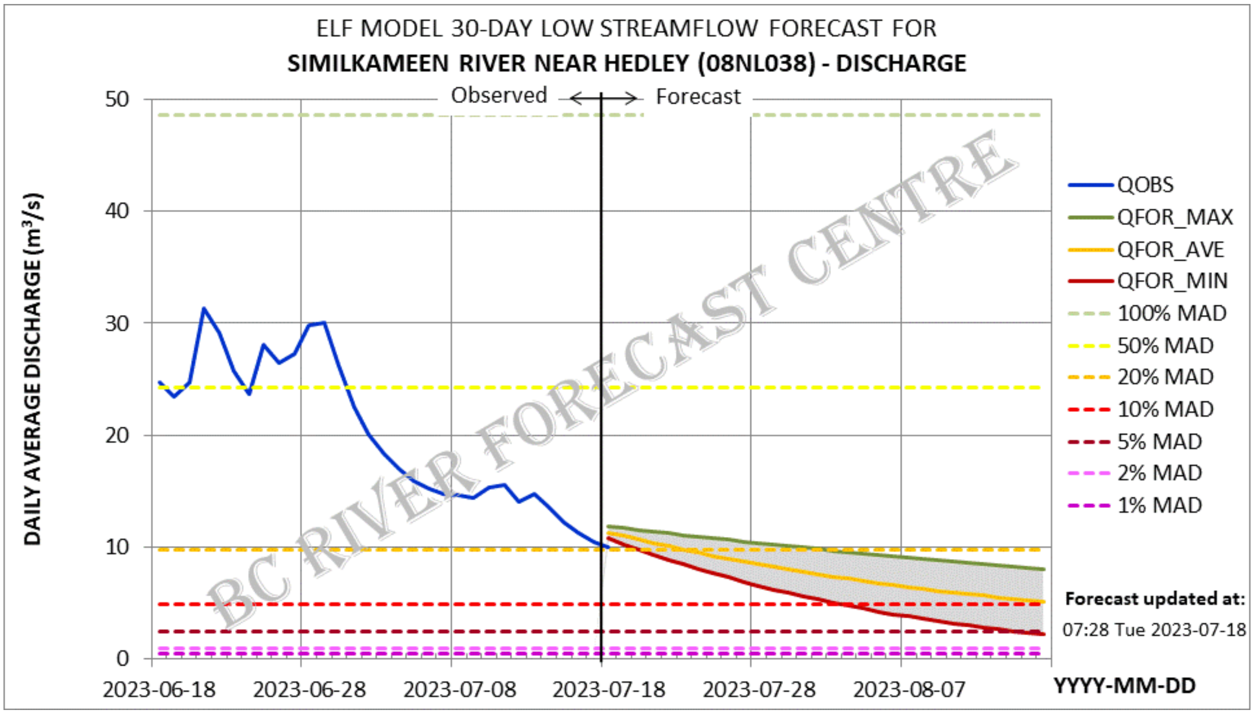

(a) Linear discharge

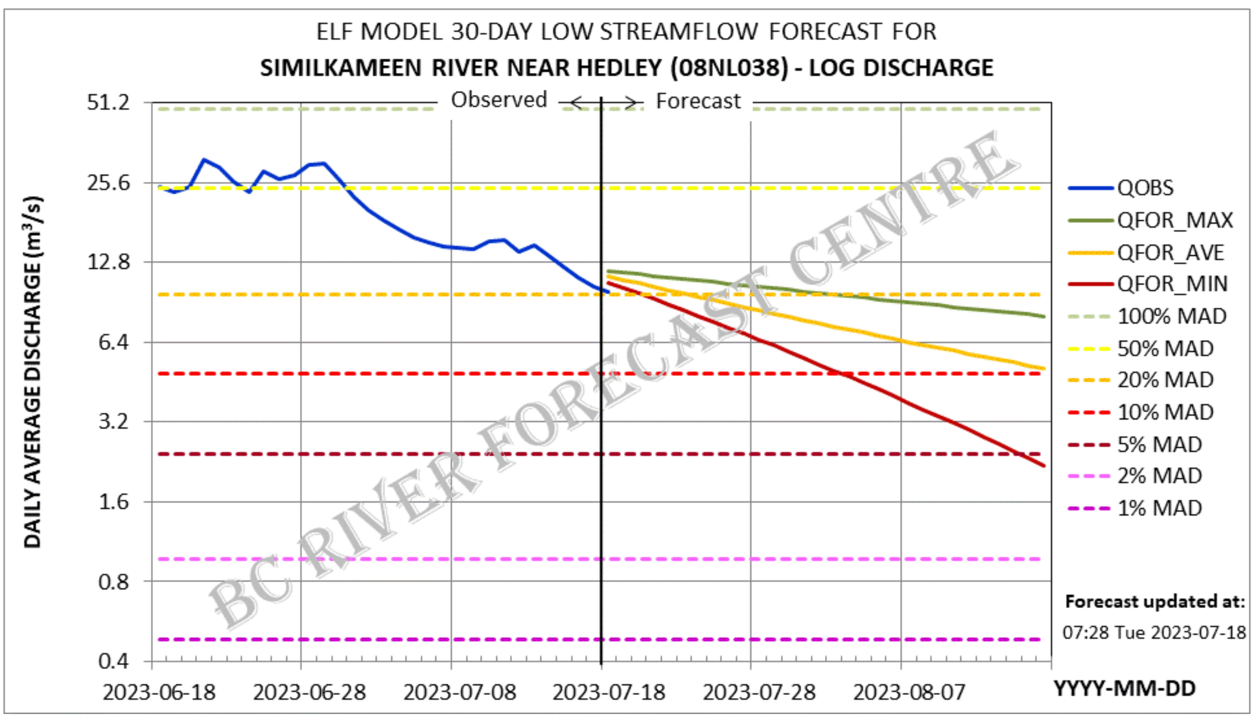

(b) Logarithmic discharge

Figure 8. Static charts of ELF Model forecast – SIMILKAMEEN RIVER NEAR HEDLEY (08NL038) (continued on next page.)

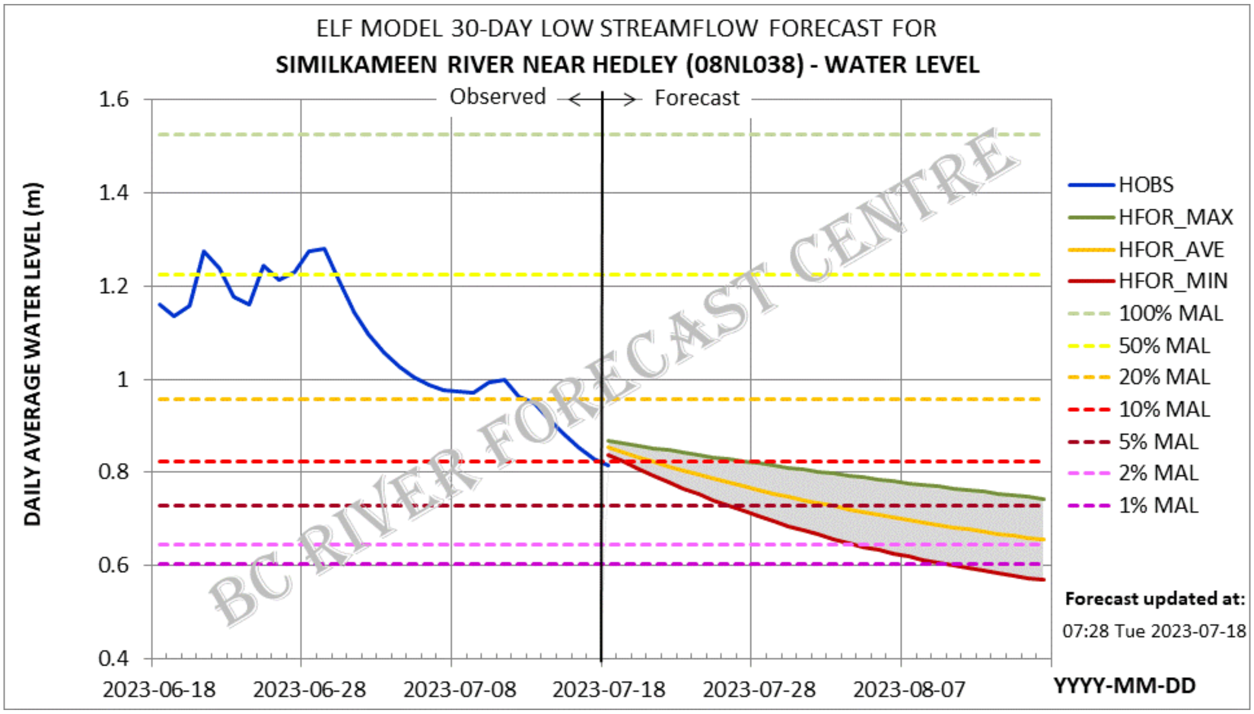

(c) Linear water level

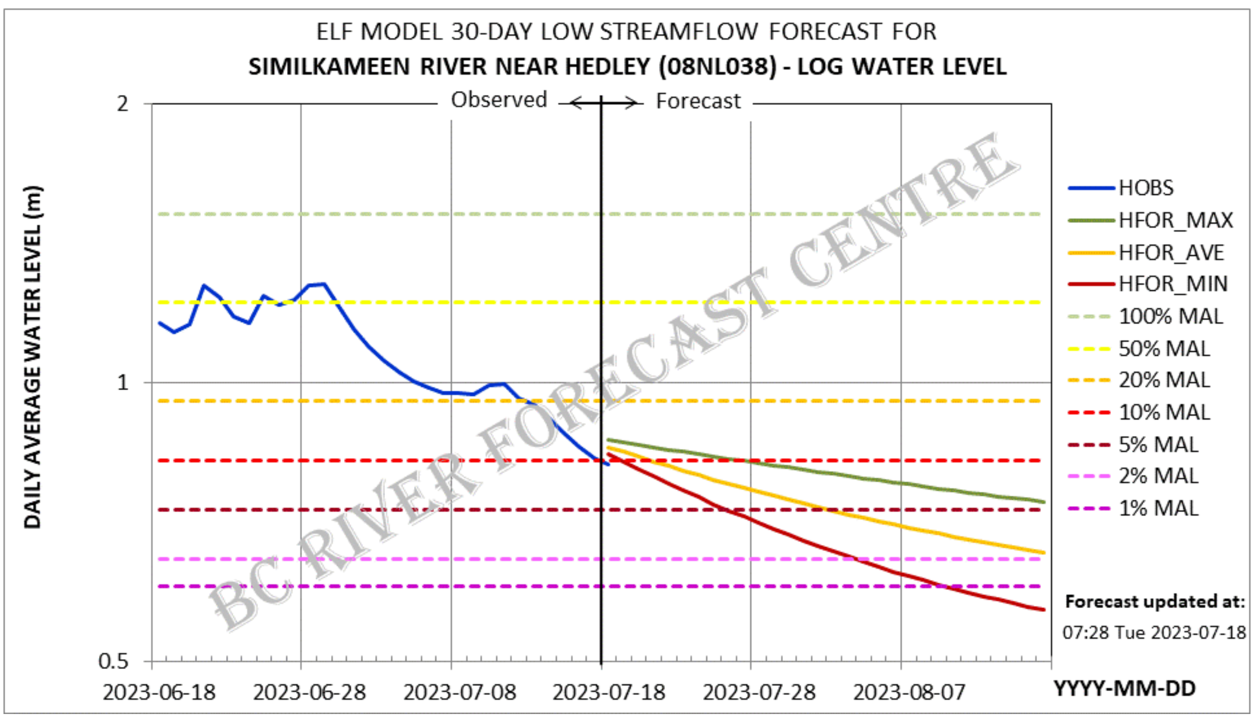

(d) Logarithmic water level

Figure 8. Static charts of ELF Model forecast – SIMILKAMEEN RIVER NEAR HEDLEY (08NL038) (continued.)

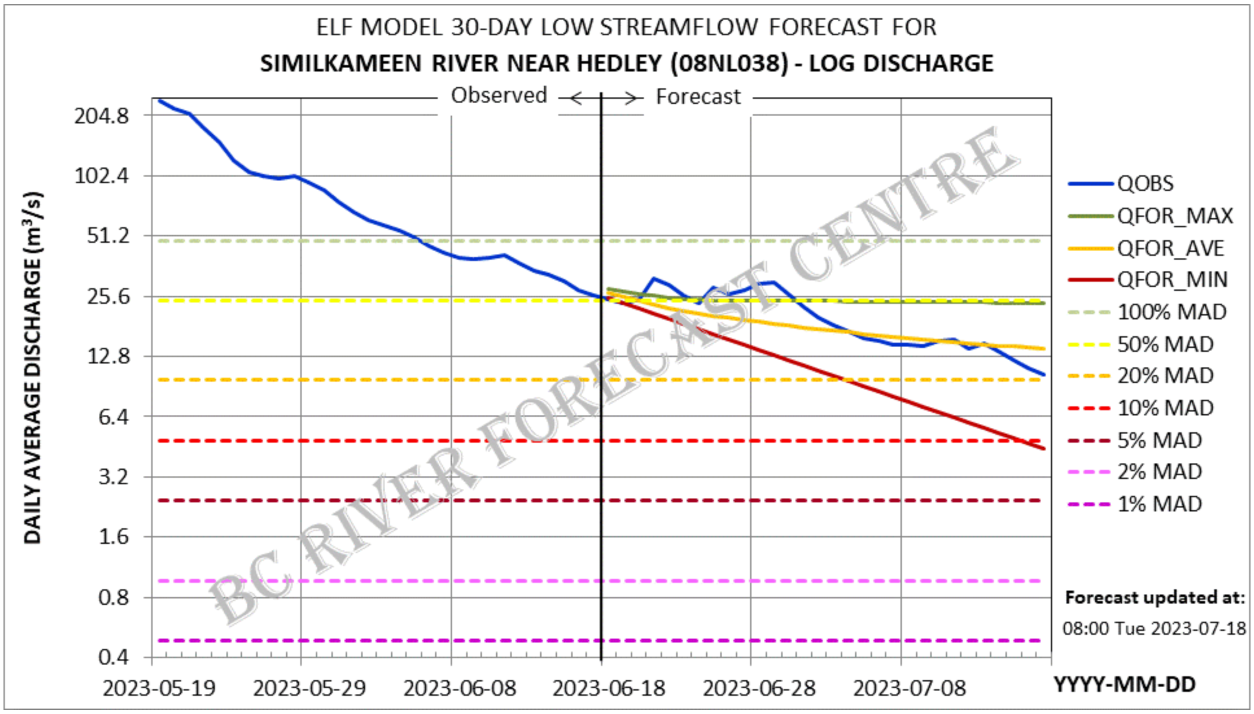

(a) Logarithmic discharge

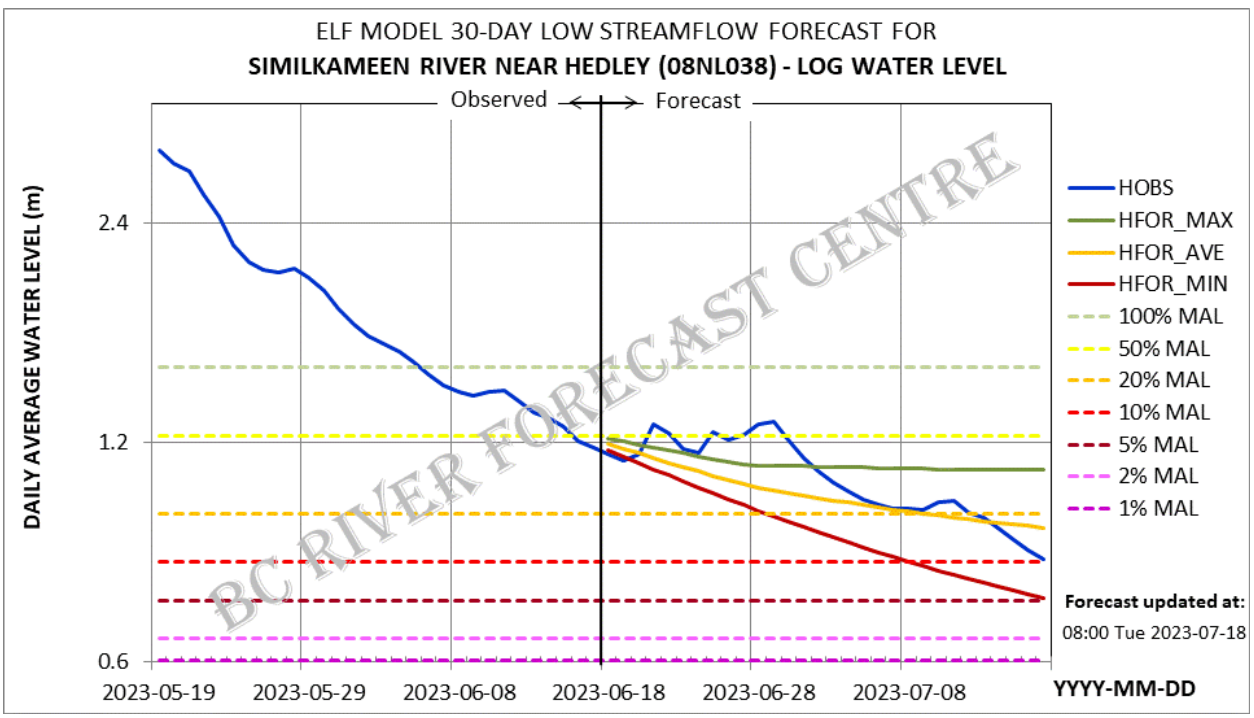

(b) Logarithmic water level

Figure 9. Static charts of verification of ELF Model forecast for previous month – SIMILKAMEEN RIVER NEAR HEDLEY (08NL038)

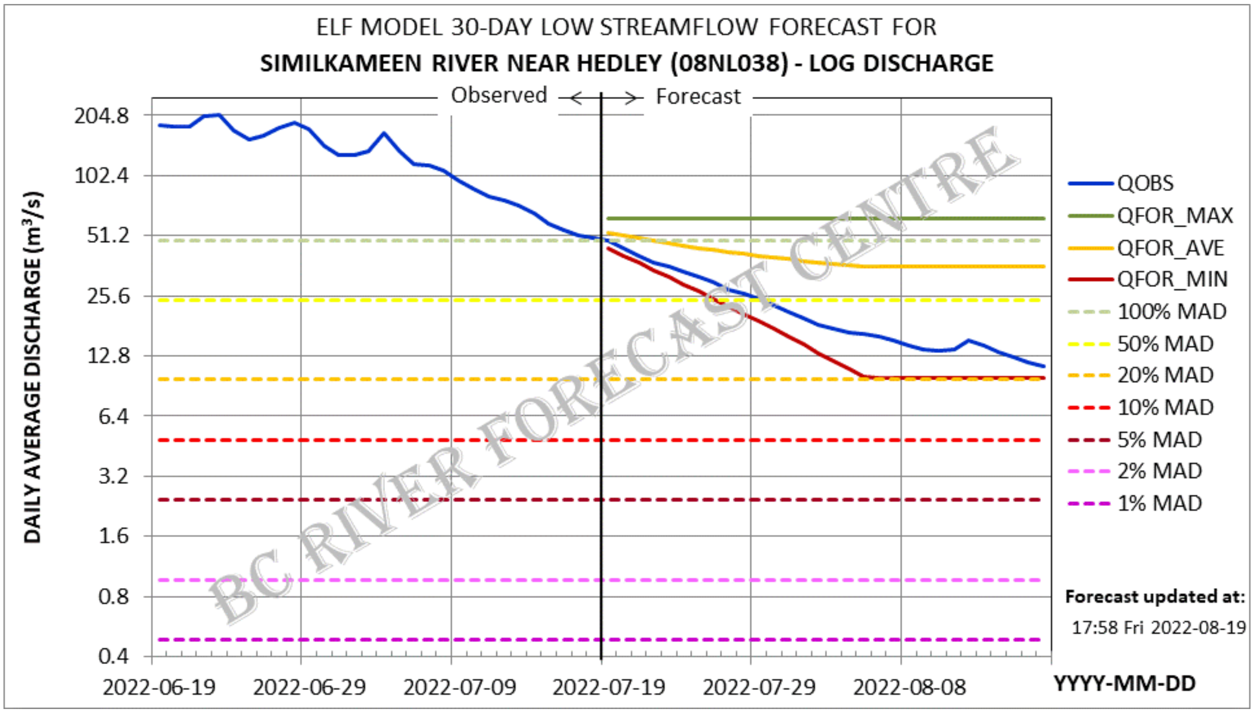

(a) Logarithmic discharge

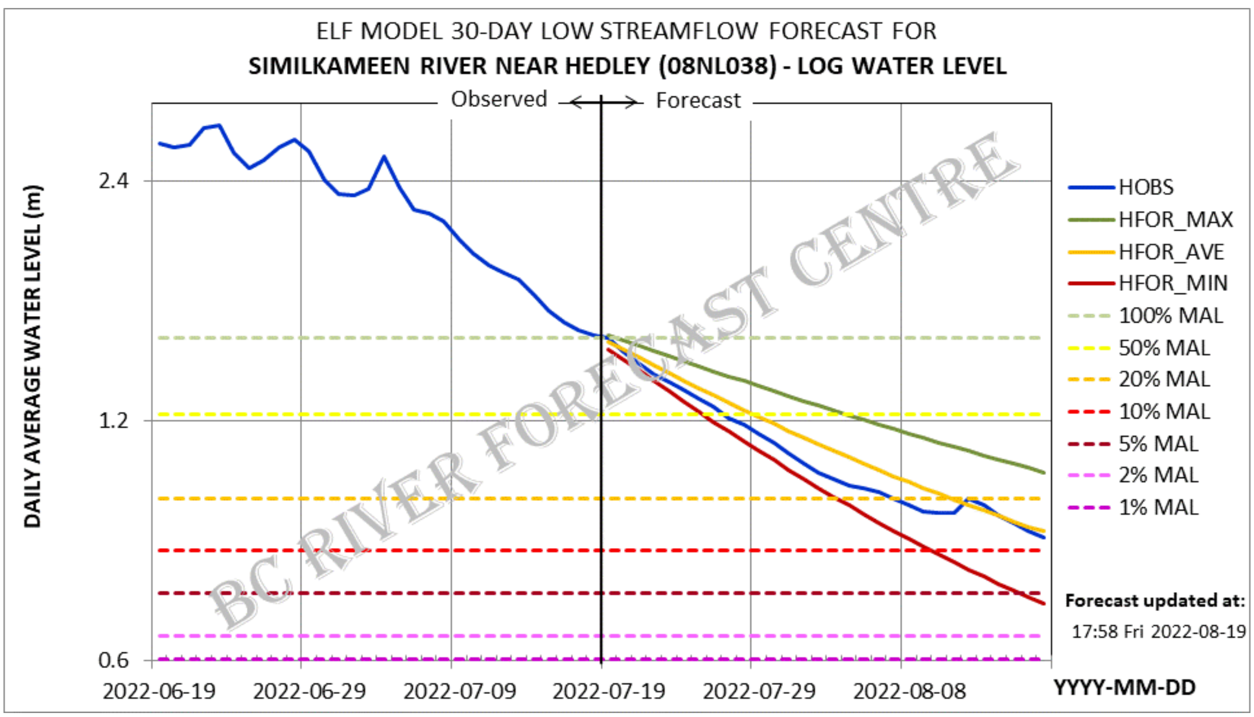

(b) Logarithmic water level

Figure 10. Static charts of verification of ELF Model forecast for a similar period in previous year – SIMILKAMEEN RIVER NEAR HEDLEY (08NL038)

9. Evaluation of ELF Model forecast accuracy

The ELF Model forecasts are analogues to ensemble forecasts and traditional statistical methods may not be appropriate for forecast accuracy evaluation. Meanwhile, the ELF Model forecasts are low flows, which's magnitude is very small or close to zero in some cases. Using the traditional statistical equations originally for flood forecast accuracy evaluation such as used in the CLEVER Model (Luo, 2015; Luo, 2021) for low flow forecast accuracy evaluation would give unfair results which may include significant bias. In these evaluation equations, any noises in the observed flow data triggered by rainfall events may result in significant errors due to the very small denominators in the evaluation equations.

In this study, a different approach is employed to evaluate the model forecast accuracy – how the forecast maximums and the minimums accommodate the observed flows. The forecast is said accurate if one of the following conditions is fulfilled.

(1) The forecast is first said accurate if all the observed flows (daily discharges or water levels) fall in between the forecast maximums and minimums in the 30-day forecast period (Figure 11 (a)).

(2) Two thirds (2/3) of the observed data points (daily discharges or water levels) fall in between the forecast maximums (+10%) and minimums (-10%). In this study, there is a total of 30 days of forecast at a daily interval, therefore the forecast is said accurate if 20 observed flows fall in between the forecast maximums (+10%) and minimums (-10%) (Figure 11 (b)).

(3) One third (1/3) of the observed data points (daily discharges or water levels), which are the lowest during the forecast period, fall in between the forecast maximums (+10%) and minimums (-10%). There is a total of 30 days of forecast in this study, therefore the forecast is said accurate if the 10 lowest observed flows fall in between the forecast maximums (+10%) and minimums (-10%) (Figure 11 (c)). This is because the ELF Model is a low flow forecasting model, and the accurate forecasts of the lowest flow are more important.

(4) Three fifths (3/5) out of the last 5 observed data points (daily discharges or water levels) fall in between the forecast maximums (+10%) and minimums (-10%). This means that the forecast is said accurate if 3 days of the observed flows in the last 5 days of the 30-day forecast period fall in between the forecast maximums (+10%) and minimums (-10%) (Figure 11 (d)). This is because the ELF Model is aiming at the medium-term (30-day) low flow forecast, and the forecasts for the latest days are more important.

For water levels, the 10% increase to the forecast maximums or decrease to the forecast minimums is calculated with the forecast water level subtracting the historical minimum water level (H_{min}), and the 10% increase or decrease must not exceed 10 cm.

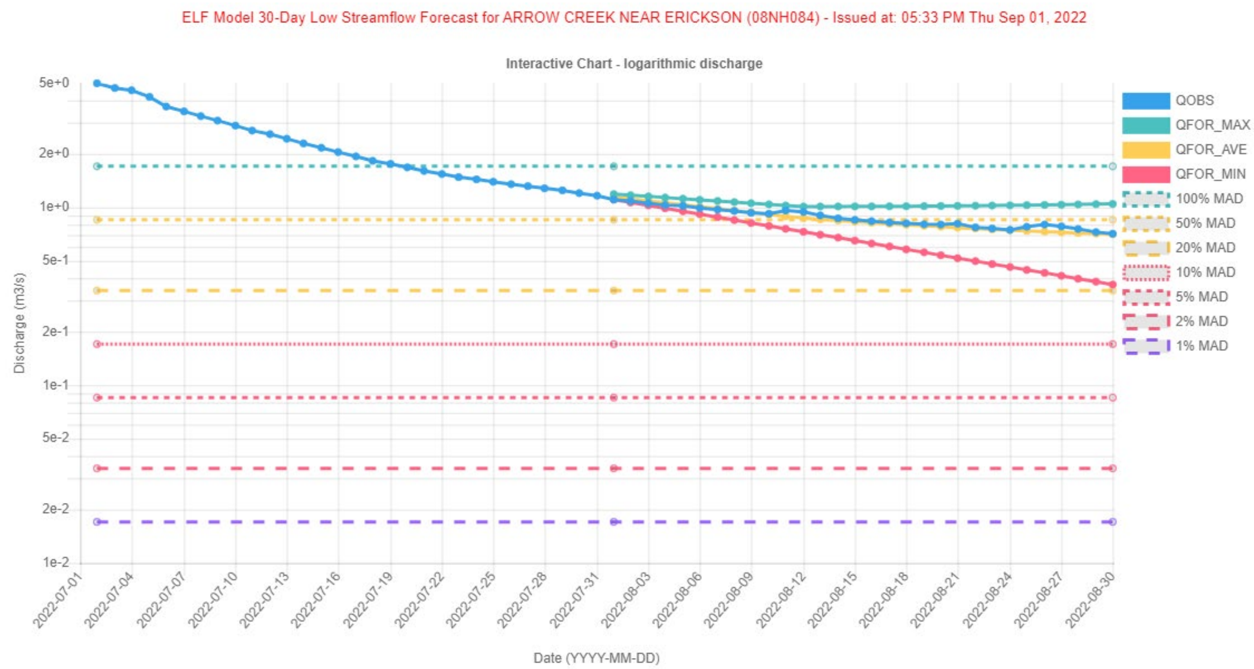

(a) All observed flows falling in between forecast maximums and minimums

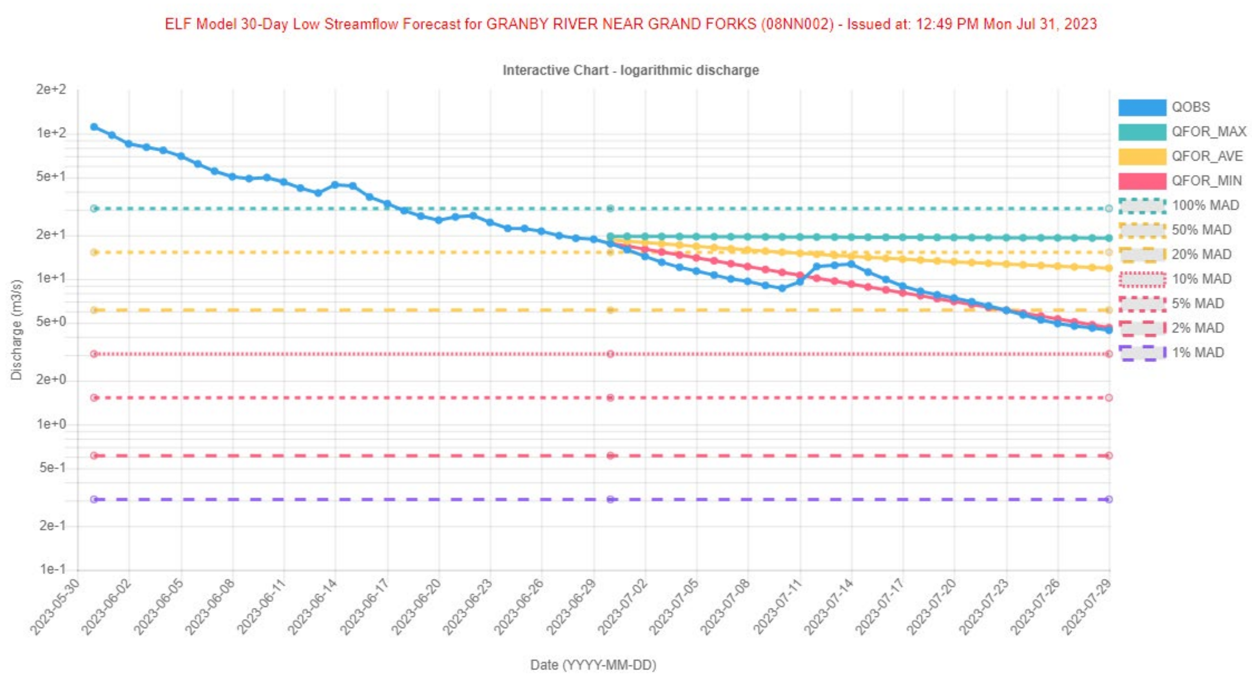

(b) 2/3 or 20 of observed data points fall in between forecast maximums (+10%) and minimums (-10%)

Figure 11. Four categories of ELF Model accurate forecasts (continued on next page).

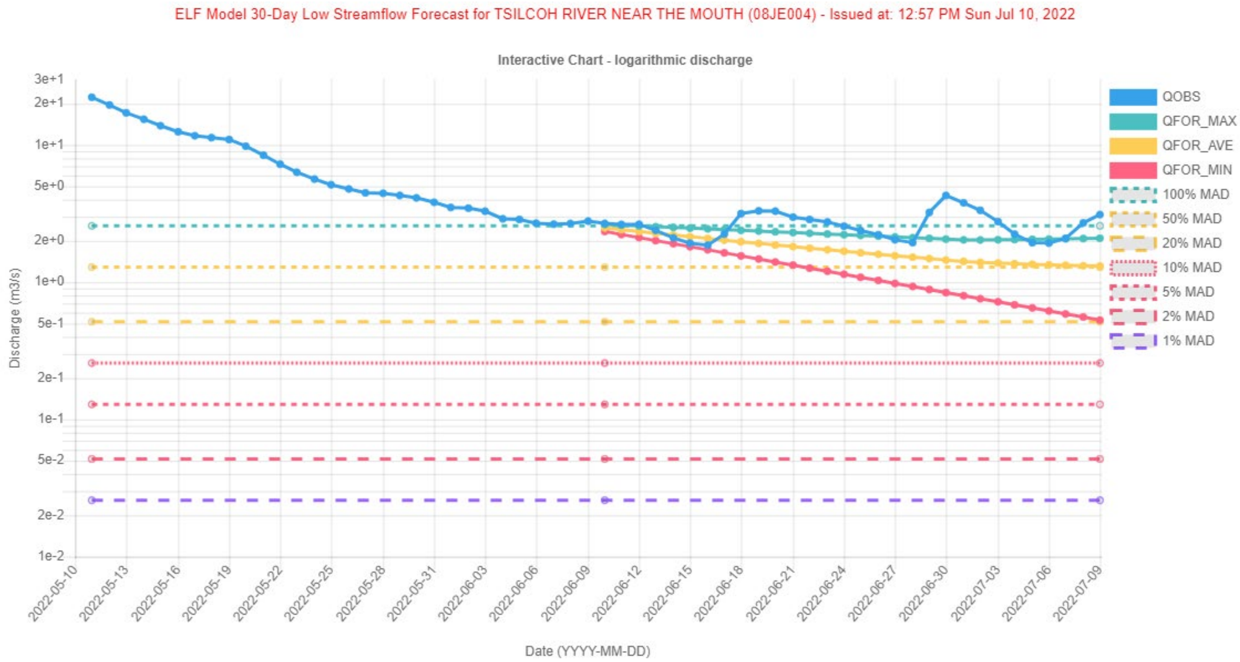

(c) 1/3 or 10 lowest observed data points out of 30 fall in between forecast maximums (+10%) and minimums (-10%)

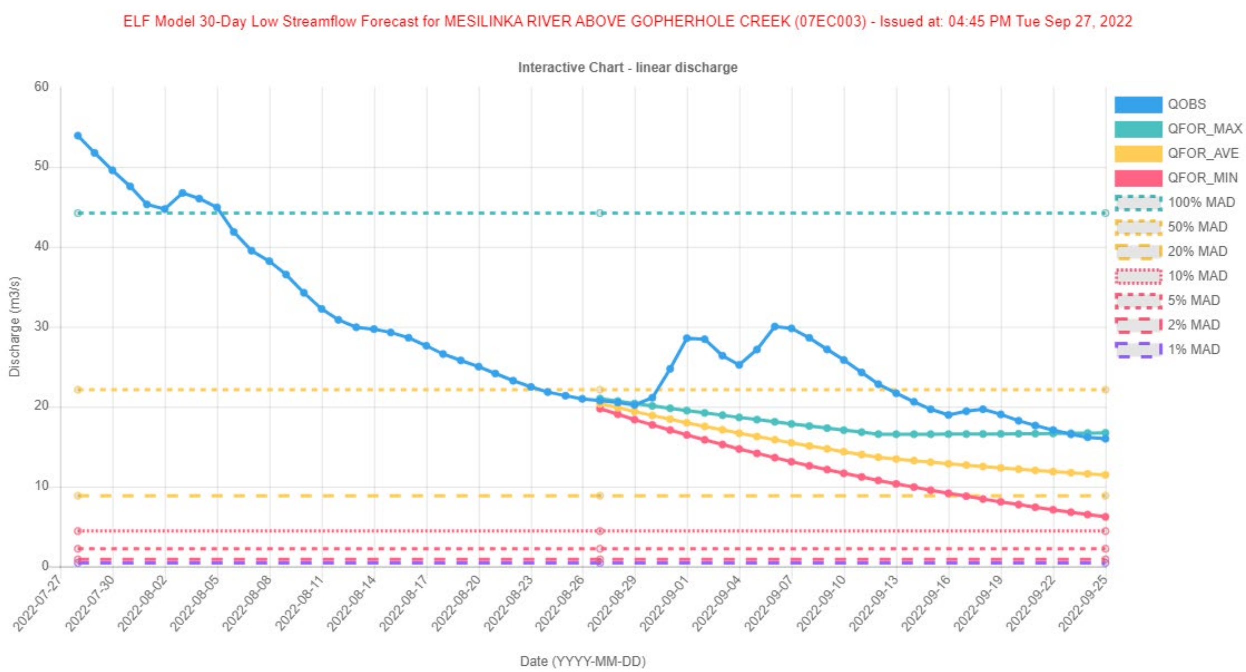

(d) 3 of last 5 observed data points fall in between forecast maximums (+10%) and minimums (-10%)

Figure 11. Four categories of ELF Model accurate forecasts (continued).

The ELF Model was put into operation as of July 2018, updating once or twice a week. Together with the reconstructed "forecasts" from January 2015 to June 2018, there is a total of 8 years of forecasts by the end of 2022 (about 800) for each of the 439 stations excluding the inactive stations. Most of these stations are WSC real-time hydrometric stations, and three of which are BC real-time water data stations.

The statistical analysis for the ELF Model all historical forecasts for all the flow stations was carried out with a program of Excel macro coded with the method described in this section. The statistical analysis opened and read about 350,000 files for the 8-year period (2015 to 2020), which made the Kamloops GIS server out of memory and consumed a total of about 40 hours of computing time of this server after the program has been optimized later.

Table 2 lists the statistics of the ELF Model historical forecast accuracy (percent of accurate forecasts) for discharge in each of the 12 months and the entire year for the 20 stations listed in Table 1 in Section 2. Figure 12 shows the statistical bar charts for two stations of the ELF Model historical forecast accuracy for discharge for two BC watersheds, the TOFINO CREEK NEAR MTHE MOUTH (08HB086) and the FRASER RIVER AT HOPE (08MF005).

From the limited number of watersheds listed in Table 2 and the two examples shown in Figure 12, it can be seen that the ELF Model historical forecast accuracy for the interior watersheds is higher than that for the coastal watersheds. This is generally true for most BC watersheds because there are more data noises in the coastal watersheds, which are incurred by rainfall events, than in the interior watersheds.

Tables 3 to 6 list the top ranked 50 stations that the ELF Model has the largest annual percent of accurate forecasts for discharges and for water levels, and that the ELF Model has largest percent of accurate forecasts in July and August for discharges and for water levels. Three phenomena can be seen form these tables. First, the ELF Model has better forecasts for water levels than for discharges. The reason for this may be that the data quality of discharges is lower than that of water levels in the low flow period because the discharge data is derived from the water level data using rating curves, which may introduce additional errors to the discharge data. In the low flow period, the flow cross section shrinks acceleratingly, which could result in an inaccurate rating curve. Second, many lake stations are included in the top ranked 50 stations. This may be because the lake effects can smooth the data and errors, daily lake water level changes are insignificant, and lake water level measurements are easier and thus the readings are more reliable. And third, more interior stations than coastal stations are include in the top ranked 50 stations for the reason given above.

Table 2. Statistics of ELF Model historical forecast accuracy for discharge for 10 coastal watersheds and 10 interior watersheds.

STATION ID	STATION NAME	PERCENT (%) OF ELF MODEL ACCURATE FORECASTS FOR DISCHARGES													TTL NO OF FOR
		JAN	FEB	MAR	APR	MAY	JUN	JUL	AUG	SEP	OCT	NOV	DEC	ANN	
08HB086	TOFINO CREEK NEAR THE MOUTH	48.1	43.3	54.4	50.9	58.3	37.7	24.2	53.3	38.0	54.5	54.9	46.7	46.1	830
08GB013	CLOWHOM RIVER NEAR CLOWHOM LAKE	48.1	60.0	49.1	29.1	40.3	64.9	57.1	49.3	53.7	46.5	57.7	76.0	53.5	838
08MH147	STAVE RIVER ABOVE STAVE LAKE	55.8	55.0	54.4	25.5	38.9	57.1	59.3	53.3	57.3	59.2	63.4	76.0	55.4	838
08GF007	WAKEMAN RIVER BELOW ATWAYKELLESSE RIVER	53.8	63.3	49.1	36.4	38.9	68.8	69.2	62.7	58.5	35.2	56.3	69.3	56.1	838
08GA071	ELAHO RIVER NEAR THE MOUTH	65.4	56.7	28.1	14.5	30.6	54.5	61.5	41.3	57.3	64.8	76.1	78.7	53.6	838
08GE002	KLINAKLINI RIVER EAST CHANNEL (MAIN) NEAR THE MOUTH	63.5	73.3	49.1	10.9	27.8	33.8	71.4	61.3	52.4	73.2	69.0	61.3	54.7	838
08CG001	ISKUT RIVER BELOW JOHNSON RIVER	51.9	50.9	70.6	14.8	15.3	61.0	58.2	60.0	65.9	64.8	57.7	54.7	52.9	824
08DB001	NASS RIVER ABOVE SHUMAL CREEK	75.0	63.3	52.6	10.9	30.6	61.0	57.1	64.0	65.9	53.5	57.7	78.7	56.6	838
08CE001	STIKINE RIVER AT TELEGRAPH CREEK	59.6	66.7	86.0	12.2	15.3	54.5	65.9	37.3	52.4	50.7	63.4	36.0	50.2	832
08EF001	SKEENA RIVER AT USK	61.5	66.7	52.6	9.1	29.2	55.8	75.8	62.7	59.8	64.8	69.0	56.0	56.4	838
08NJ026	DUHAMEL CREEK ABOVE DIVERSIONS	71.2	61.7	22.8	9.1	25.0	36.4	70.3	82.7	63.4	53.5	52.1	74.7	53.3	838
08NG077	ST. MARY RIVER BELOW MORRIS CREEK	82.1	54.5	54.5	16.7	46.7	35.9	76.1	86.0	34.5	69.6	59.6	51.0	56.0	493
08NF001	KOOTENAY RIVER AT KOOTENAY CROSSING	73.1	60.0	60.0	14.5	33.3	51.9	68.1	76.0	62.2	78.9	67.6	58.7	59.4	836
08NG002	BULL RIVER NEAR WARDNER	67.3	70.0	24.6	12.7	51.4	46.8	76.9	93.3	70.7	67.6	67.6	82.7	62.9	838
08NN026	KETTLE RIVER NEAR WESTBRIDGE	75.0	60.0	20.0	9.4	33.3	51.9	65.9	80.0	46.3	46.5	53.5	66.7	52.0	834
08NL038	SIMILKAMEEN RIVER NEAR HEDLEY	42.3	53.3	38.6	14.5	43.1	50.6	80.2	86.7	50.0	38.0	42.3	54.7	51.4	838
08NG065	KOOTENAY RIVER AT FORT STEELE	71.2	63.3	59.6	12.7	29.2	53.2	75.8	89.3	69.5	74.6	67.6	64.0	62.1	838
08LF051	THOMPSON RIVER NEAR SPENCES BRIDGE	78.8	82.1	64.9	18.2	37.5	59.7	52.7	88.0	61.0	76.1	70.4	88.0	64.9	834
08MC018	FRASER RIVER NEAR MARGUERITE	71.2	51.7	59.3	28.3	47.2	59.7	68.1	80.0	62.2	59.2	62.0	78.7	61.6	833
08MF005	FRASER RIVER AT HOPE	69.2	73.3	45.6	27.3	33.3	63.6	56.0	84.0	63.4	78.9	59.2	74.7	61.3	838

Note: ANN – annual, TTL NO OF FOR – total number of forecasts.

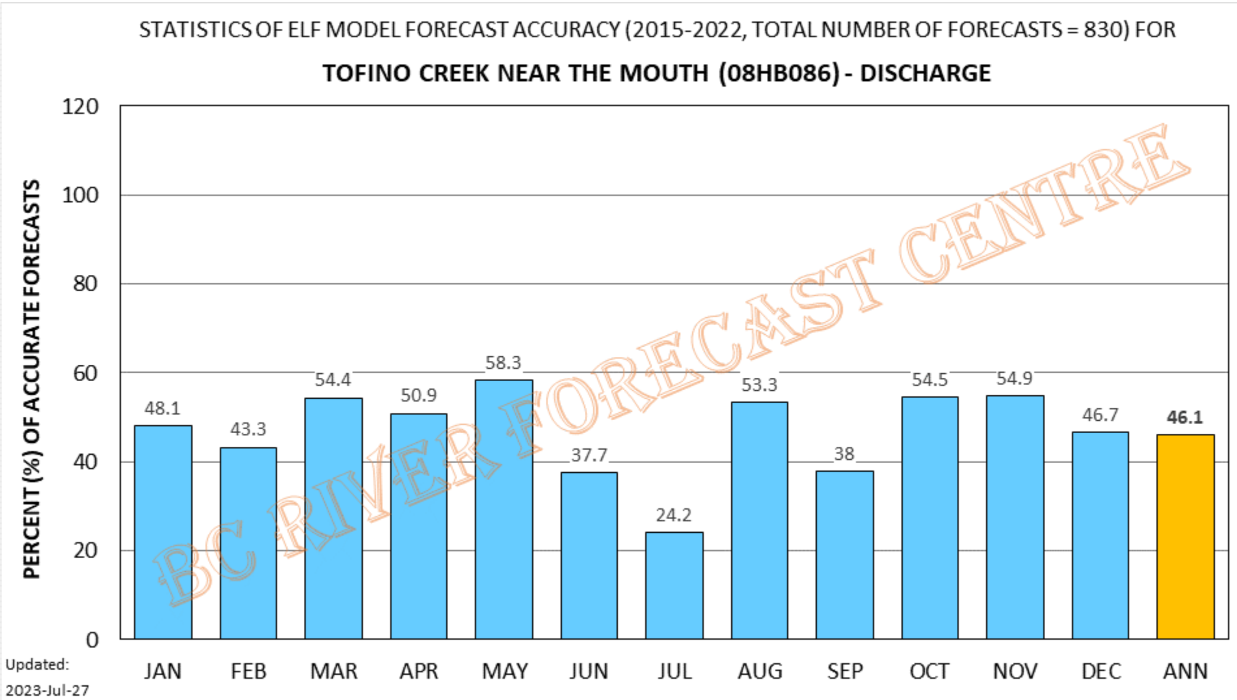

(a) TOFINO CREEK NEAR THE MOUTH (08HB086)

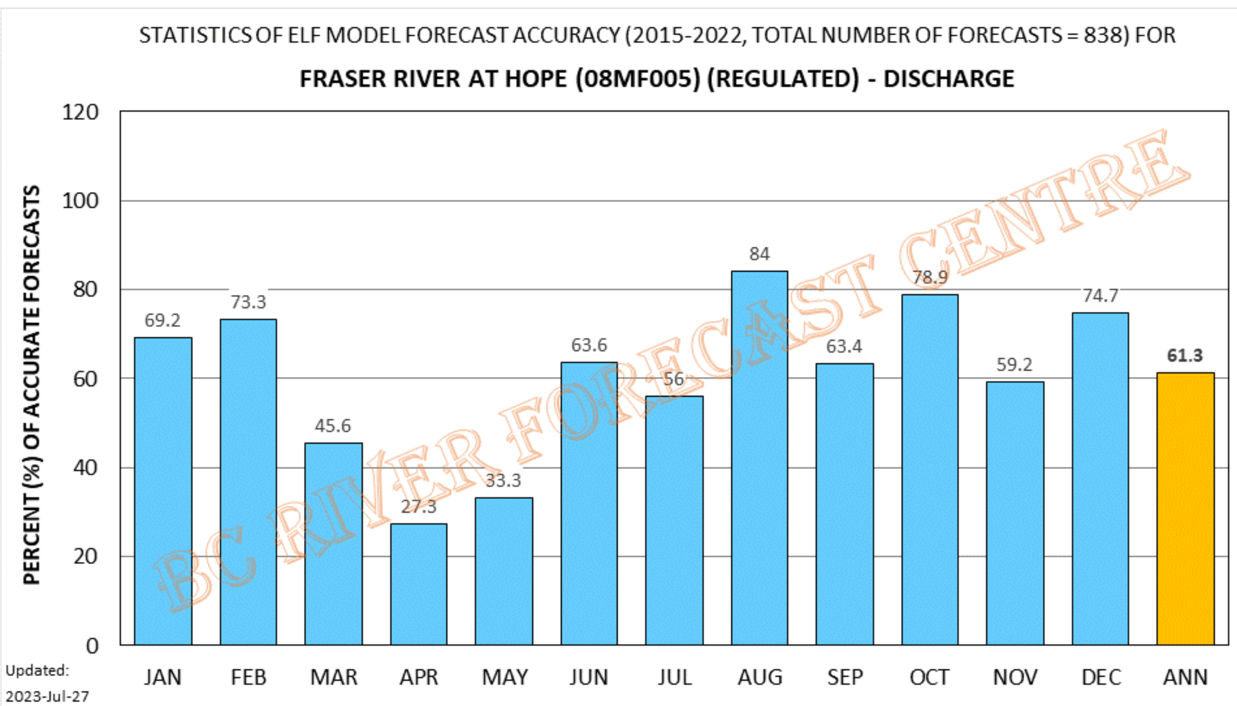

(b) FRASER RIVER AT HOPE (08MF005)

Figure 12. Statistical bar charts of ELF Model historical forecast accuracy for discharge for two BC watersheds.

Table 3. Top ranked 50 stations ELF Model has largest annual percent of accurate forecasts for discharges (Note: RK – rank, ANN – annual, JL+AG – July and August).

RK	STATION ID	STATION NAME	PERCENT (%) OF ELF MODEL ACCURATE FORECASTS FOR DISCHARGES													
			JAN	FEB	MAR	APR	MAY	JUN	JUL	AUG	SEP	OCT	NOV	DEC	ANN	JL+AG
1	08JE001	STUART RIVER NEAR FORT ST. JAM	92	98	91	13	3	62	81	99	100	94	93	97	77.8	90.0
2	08EC013	BABINE RIVER AT OUTLET OF NILK	92	93	83	16	39	68	88	88	93	78	85	91	77.0	88.0
3	08HD021	QUINSAM RIVER AT ARGONAUT B	71	83	95	55	71	82	88	93	83	41	61	51	73.2	90.6
4	08JB002	STELLAKO RIVER AT GLENANNAN	90	88	84	16	46	68	64	89	89	69	73	91	72.7	76.5
5	08ME029	BRIDGE RIVER BELOW LAJOIE DAM	79	86	91	70	48	64	80	70	31	60	89	100	70.8	74.9
6	08NK022	LINE CREEK AT THE MOUTH	79	69	73	32	35	53	82	88	95	83	66	75	70.6	85.0
7	10BE009	TEETER CREEK NEAR THE MOUTH	84	72	71	42	61	69	75	72	63	65	66	79	68.3	73.4
8	08NM002	OKANAGAN RIVER AT OKANAGAN	75	40	58	69	50	69	62	65	76	82	85	79	67.7	63.4
9	08LE108	EAST CANOE CREEK ABOVE DAM	64	69	27	13	67	85	77	96	60	76	68	69	67.5	86.7
10	09AA001	ATLIN LAKE AT ATLIN	91	93	100	100	18	0	34	77	60	79	98	88	67.5	55.6
11	08LF033	THOMPSON RIVER NEAR SAVONA	0	100	56	50	21	64	54	100	67	86	90	88	67.3	76.9
12	08NM085	OKANAGAN RIVER NEAR OLIVER	71	48	61	56	51	68	68	64	71	78	85	77	67.1	66.1
13	09AA013	TUTSHI RIVER AT OUTLET OF TUTS	75	92	81	64	15	52	68	75	66	63	83	79	67.0	71.4
14	08NM247	OKANAGAN RIVER BELOW MCINT	69	45	63	64	63	61	63	67	66	75	85	81	66.9	64.7
15	08LD001	ADAMS RIVER NEAR SQUILAX	96	90	70	18	21	62	56	93	73	78	63	83	66.8	74.7
16	08LB024	FISHTRAP CREEK NEAR MCLURE	61	67	42	31	79	74	76	84	64	72	55	67	66.7	80.1
17	08JB003	NAUTLEY RIVER NEAR FORT FRASE	65	83	51	9	50	68	70	91	95	63	63	67	66.3	80.5
18	08MH024	FRASER RIVER AT MISSION	75	73	79	35	38	57	58	91	78	75	69	63	65.9	74.5
19	08LE031	SOUTH THOMPSON RIVER AT CHA	83	78	68	29	17	57	59	93	84	79	59	79	65.8	76.3
20	08EE020	TELKWA RIVER BELOW TSAI CREEK	89	83	75	11	24	68	70	65	77	65	73	84	65.8	67.8
21	08ME002	CAYOOSH CREEK NEAR LILLOOET	75	68	75	47	29	51	58	73	81	78	72	79	65.4	65.8
22	08MH005	ALOUETTE RIVER NEAR HANEY	48	65	65	47	60	68	97	92	67	55	47	55	65.3	94.4
23	08NH016	DUCK CREEK NEAR WYNNDEL	87	67	55	25	30	42	79	81	82	54	80	90	65.3	80.0
24	08NK018	FORDING RIVER AT THE MOUTH	79	78	70	15	26	49	75	76	87	87	65	65	65.2	75.4
25	08LF051	THOMPSON RIVER NEAR SPENCES	79	82	65	18	38	60	53	88	61	76	70	88	64.9	70.4
26	08NH084	ARROW CREEK NEAR ERICKSON	67	68	42	22	29	57	88	89	76	68	66	83	64.8	88.6
27	10BE013	SMITH RIVER NEAR THE MOUTH	80	53	52	62	80	68	85	68	85	63	27	43	64.8	76.3
28	08KH006	QUESNEL RIVER NEAR QUESNEL	79	67	60	24	39	71	55	92	62	73	69	80	64.7	73.5
29	08JA017	NECHAKO RIVER BELOW CHESLAT	85	87	68	36	54	68	43	35	79	65	73	89	64.6	38.8
30	07ED001	NATION RIVER NEAR FORT ST. JAM	0	38	100	63	7	9	77	100	100	100	90	63	64.5	88.5
31	08ME025	YALAKOM RIVER ABOVE ORE CREE	55	71	93	23	27	48	70	83	81	83	64	65	64.4	76.1
32	08KA007	FRASER RIVER AT RED PASS	94	88	83	29	14	48	63	79	56	75	68	84	64.2	70.7
33	08ME003	SETON RIVER NEAR LILLOOET	94	78	84	46	56	47	52	60	31	85	90	69	64.2	55.8
34	08KH001	QUESNEL RIVER AT LIKELY	89	90	65	27	21	62	50	92	66	69	58	85	64.1	70.8
35	08LF099	ARROWSTONE CREEK NEAR THE M	71	93	50	23	63	43	67	57	86	59	76	75	64.1	61.8
36	08NK016	ELK RIVER NEAR NATAL	73	67	67	12	18	43	73	83	94	93	63	65	64.0	78.0
37	08NM037	SHATFORD CREEK NEAR PENTICTO	92	82	43	15	29	49	84	91	57	49	79	87	63.9	87.1
38	08NM050	OKANAGAN RIVER AT PENTICTON	64	42	67	75	42	64	67	69	65	55	82	73	63.7	68.2
39	08NB016	SPLIT CREEK AT THE MOUTH	93	89	91	45	19	49	44	78	66	78	57	82	63.7	61.2
40	08NL076	EWART CREEK NEAR CATHEDRAL P	87	83	69	4	27	49	72	88	59	60	74	84	63.6	80.1
41	08LC002	SHUSWAP RIVER NEAR ENDERBY	94	80	51	29	22	44	64	89	70	70	65	81	63.4	76.5
42	08MG001	CHEHALIS RIVER NEAR HARRISON	80	50	67	63	29	36	85	100	80	43	40	72	63.3	92.3
43	07FD010	PEACE RIVER ABOVE ALCES RIVER	60	67	72	55	50	52	65	65	61	62	72	79	63.2	65.1
44	08LC003	SHUSWAP RIVER NEAR LUMBY	94	75	54	20	25	46	62	73	66	78	73	91	63.1	67.4
45	08MF040	FRASER RIVER ABOVE TEXAS CREE	73	67	51	26	40	69	65	84	65	82	62	64	63.0	74.4
46	08NG002	BULL RIVER NEAR WARDNER	67	70	25	13	51	47	77	93	71	68	68	83	62.9	85.1
47	08HD005	QUINSAM RIVER NEAR CAMPBELL	52	58	72	75	76	70	84	85	45	39	49	45	62.9	84.4
48	08NJ160	LEMON CREEK ABOVE SOUTH LEM	81	65	68	9	25	43	85	84	59	70	73	81	62.9	84.3
49	08NH005	KASLO RIVER BELOW KEMP CREEK	87	65	51	11	26	47	70	85	60	80	75	87	62.8	77.8
50	08LC018	SHUSWAP RIVER AT OUTLET OF SU	96	63	63	29	21	46	53	75	65	78	79	91	62.8	63.7

Table 4. Top ranked 50 stations ELF Model having largest annual percent of accurate forecasts for water levels (Note: RK – rank, ANN – annual, JL+AG – July and August).

	STATION		PERCENT (%) OF ELF MODEL ACCURATE FORECASTS FOR WATER LEVELS													
RK	ID	STATION NAME	JAN	FEB	MAR	APR	MAY	JUN	JUL	AUG	SEP	OCT	NOV	DEC	ANN	JL+AG
1	08NM084	SKAHA LAKE AT OKANAGAN FALLS	100	98	98	87	94	83	98	99	94	100	100	100	95.9	98.3
2	08NM143	KALAMALKA LAKE AT VERNON PUM	100	100	98	78	68	92	93	100	96	97	100	100	93.7	96.7
3	08EC003	BABINE LAKE AT TOPLEY LANDING	100	82	91	38	40	70	90	99	93	100	99	100	84.1	94.4
4	08NM083	OKANAGAN LAKE AT KELOWNA	100	83	86	40	38	77	80	97	100	97	99	100	83.7	88.8
5	08NL076	EWART CREEK NEAR CATHEDRAL PA	98	87	92	33	50	66	81	99	84	88	95	97	81.2	89.9
6	08LF099	ARROWSTONE CREEK NEAR THE MO	82	89	61	48	71	70	86	67	98	96	92	90	80.7	76.6
7	08HD021	QUINSAM RIVER AT ARGONAUT BR	85	83	97	56	78	91	95	97	90	51	69	60	79.8	95.9
8	08JB007	NADINA LAKE NEAR NORALEE	100	90	84	40	53	79	84	89	78	68	78	84	77.3	86.4
9	08LG046	NICOLA LAKE NEAR NICOLA	100	60	75	44	26	84	62	87	100	92	93	99	77.2	74.1
10	08EC001	BABINE RIVER AT BABINE	90	100	93	24	38	66	87	88	89	75	80	87	76.8	87.4
11	10BE009	TEETER CREEK NEAR THE MOUTH	88	78	86	56	71	79	78	77	83	80	68	76	76.8	77.7
12	08NB016	SPLIT CREEK AT THE MOUTH	86	89	100	55	35	83	55	84	90	80	89	82	76.5	69.4
13	08GE003	ICY CREEK NEAR THE MOUTH	83	80	74	49	71	69	97	73	79	76	69	77	75.5	85.0
14	08JB003	NAUTLEY RIVER NEAR FORT FRASE	75	90	58	24	67	74	80	97	96	70	70	75	74.6	88.8
15	08NM002	OKANAGAN RIVER AT OKANAGAN F	77	55	65	73	61	78	77	72	76	86	85	81	74.2	74.5
16	08NK022	LINE CREEK AT THE MOUTH	71	61	82	32	35	59	92	86	100	91	77	67	73.4	89.4
17	08JB002	STELLAKO RIVER AT GLENANNAN	83	87	63	18	54	75	76	89	85	61	70	83	71.5	82.6
18	08MH005	ALOUETTE RIVER NEAR HANEY	54	67	75	58	67	70	95	97	78	66	49	63	71.2	95.9
19	08NL050	HEDLEY CREEK NEAR THE MOUTH	89	85	69	35	74	71	79	85	63	56	75	68	71.0	82.2
20	08LG008	SPIUS CREEK NEAR CANFORD	80	69	82	51	44	65	79	93	75	65	63	78	70.6	85.8
21	08KG001	WEST ROAD RIVER NEAR CINEMA	81	89	62	34	61	71	66	90	69	79	63	78	70.3	78.1
22	08ME029	BRIDGE RIVER BELOW LAJOIE DAM	65	74	72	68	39	75	90	84	31	55	87	98	70.1	87.3
23	08NM065	VERNON CREEK AT OUTLET OF KALA	77	83	77	62	39	79	63	67	66	73	78	83	70.0	64.7
24	08NG002	BULL RIVER NEAR WARDNER	67	73	44	22	53	53	80	96	84	76	79	85	69.6	88.1
25	08NK030	ELK RIVER BELOW ELKO DAM	75	57	61	35	44	52	80	93	89	85	75	73	69.6	86.8
26	08NM050	OKANAGAN RIVER AT PENTICTON	73	50	72	75	50	73	68	75	68	69	80	77	69.2	71.4
27	08LF002	BONAPARTE RIVER BELOW CACHE (	77	65	53	46	71	46	70	89	84	89	69	63	69.1	79.8
28	07FA003	HALFWAY RIVER ABOVE GRAHAM I	83	74	77	67	39	73	76	80	87	83	30	63	69.1	77.9
29	08NM243	VASEUX LAKE NEAR THE OUTLET	81	77	81	55	60	64	74	48	63	63	83	85	69.1	60.8
30	08LE108	EAST CANOE CREEK ABOVE DAM	68	75	39	13	67	79	77	90	69	65	57	88	68.6	83.8
31	08JA023	NECHAKO RESERVOIR AT SKINS LAK	100	88	79	53	1	35	42	96	89	78	89	85	68.3	68.9
32	08HB084	PUNTLEDGE RIVER BELOW DIVERS	38	69	69	61	83	86	75	70	41	70	64	78	67.9	72.3
33	08LF027	DEADMAN RIVER ABOVE CRISS CRE	70	69	67	29	56	72	53	86	93	72	74	64	67.8	69.2
34	08NM171	VASEUX CREEK ABOVE SOLCO CREE	87	67	51	35	51	62	77	75	73	65	78	83	67.7	75.8
35	07FB009	FLATBED CREEK AT KILOMETRE 110	75	63	74	38	63	58	78	80	73	69	72	60	67.5	79.0
36	08NM200	INKANEEP CREEK NEAR THE MOUTH	73	73	44	46	74	57	74	84	51	61	83	84	67.5	78.8
37	08MH168	OR CREEK NEAR COQUITLAM	50	68	65	75	62	73	85	85	52	65	62	60	67.4	85.0
38	08NM085	OKANAGAN RIVER NEAR OLIVER	73	58	63	60	50	69	68	63	66	78	83	76	67.4	65.4
39	08HD022	CAMPBELL RIVER AT CAMPBELL RIV	0	88	89	63	93	64	85	70	56	14	60	25	67.3	77.3
40	08HA016	BINGS CREEK NEAR THE MOUTH	52	63	74	86	96	77	91	81	52	39	52	39	67.2	86.3
41	08HF004	TSITIKA RIVER BELOW CATHERINE	63	67	60	58	73	71	79	89	57	53	64	64	67.1	83.7
42	08NM174	WHITEMAN CREEK ABOVE BOULEA	73	70	53	38	58	62	60	87	74	73	72	76	67.1	73.6
43	08KA007	FRASER RIVER AT RED PASS	96	90	88	35	19	51	67	79	59	69	75	88	67.1	72.9
44	08EC013	BABINE RIVER AT OUTLET OF NILKI	67	83	60	11	40	71	79	83	88	59	62	80	66.9	80.9
45	08JE001	STUART RIVER NEAR FORT ST. JAM	87	88	79	11	1	46	55	96	93	80	80	84	66.8	75.5
46	08ME003	SETON RIVER NEAR LILLOOET	96	78	86	51	60	57	54	64	31	83	90	72	66.8	58.9
47	08NM037	SHATFORD CREEK NEAR PENTICTON	90	80	49	25	46	52	80	89	56	62	81	83	66.7	84.8
48	08NK016	ELK RIVER NEAR NATAL	65	69	56	12	38	59	79	87	96	93	54	65	66.6	82.9
49	08HD027	QUINSAM RIVER BELOW LOWER Q	46	67	72	76	89	70	80	72	52	58	59	51	66.3	76.1
50	08ME002	CAYOOSH CREEK NEAR LILLOOET	81	72	74	47	31	60	59	71	72	78	76	79	66.2	65.0

Table 5. Top ranked 50 stations ELF Model has largest Jul + Aug percent of accurate forecasts for discharges (Note: RK – rank, ANN – annual, JL+AG – July and August).

	STATION		PERCENT (%) OF ELF MODEL ACCURATE FORECASTS FOR DISCHARGES													
RK	ID	STATION NAME	JAN	FEB	MAR	APR	MAY	JUN	JUL	AUG	SEP	OCT	NOV	DEC	ANN	JL+AG
1	08MH005	ALOUETTE RIVER NEAR HANEY	48	65	65	47	60	68	97	92	67	55	47	55	65.3	94.4
2	08NE039	BIG SHEEP CREEK NEAR ROSSLAND	65	38	20	9	33	62	86	100	71	58	68	70	59.9	93.1
3	08MG001	CHEHALIS RIVER NEAR HARRISON	80	50	67	63	29	36	85	100	80	43	40	72	63.3	92.3
4	08NE130	WHATSHAN RIVER BELOW BARNE	0	75	44	13	0	0	85	100	22	86	60	75	48.6	92.3
5	08HD021	QUINSAM RIVER AT ARGONAUT B	71	83	95	55	71	82	88	93	83	41	61	51	73.2	90.6
6	08JE001	STUART RIVER NEAR FORT ST. JAM	92	98	91	13	3	62	81	99	100	94	93	97	77.8	90.0
7	08NH084	ARROW CREEK NEAR ERICKSON	67	68	42	22	29	57	88	89	76	68	66	83	64.8	88.6
8	07ED001	NATION RIVER NEAR FORT ST. JAM	0	38	100	63	7	9	77	100	100	100	90	63	64.5	88.5
9	08HA002	COWICHAN RIVER AT LAKE COWI	40	57	63	49	51	46	79	97	57	23	56	39	55.7	88.2
10	08EC013	BABINE RIVER AT OUTLET OF NILK	92	93	83	16	39	68	88	88	93	78	85	91	77.0	88.0
11	08NM037	SHATFORD CREEK NEAR PENTICTO	92	82	43	15	29	49	84	91	57	49	79	87	63.9	87.1
12	08NL070	SIMILKAMEEN RIVER ABOVE GOO	75	75	60	9	23	49	85	89	51	44	63	73	59.2	86.9
13	08LE108	EAST CANOE CREEK ABOVE DAM	64	69	27	13	67	85	77	96	60	76	68	69	67.5	86.7
14	08MF062	COQUIHALLA RIVER BELOW NEED	58	73	58	12	32	45	85	87	49	22	63	65	55.3	86.1
15	08NG002	BULL RIVER NEAR WARDNER	67	70	25	13	51	47	77	93	71	68	68	83	62.9	85.1
16	08NK022	LINE CREEK AT THE MOUTH	79	69	73	32	35	53	82	88	95	83	66	75	70.6	85.0
17	10AB001	FRANCES RIVER NEAR WATSON LA	38	100	67	25	0	18	100	70	67	57	10	35	46.8	85.0
18	08NE087	DEER CREEK AT DEER PARK	75	57	11	8	41	49	70	100	61	46	56	78	56.9	84.8
19	08GB014	HORSESHOE RIVER ABOVE LOIS LA	40	70	58	58	74	70	81	88	48	32	45	53	60.7	84.7
20	08HD005	QUINSAM RIVER NEAR CAMPBELL	52	58	72	75	76	70	84	85	45	39	49	45	62.9	84.4
21	08NJ160	LEMON CREEK ABOVE SOUTH LEM	81	65	68	9	25	43	85	84	59	70	73	81	62.9	84.3
22	08NE074	SALMO RIVER NEAR SALMO	79	60	25	11	36	48	87	81	51	54	62	65	56.4	84.1
23	08NH139	MOYIE RIVER ABOVE NOKE CREEK	89	73	48	12	27	39	91	76	61	36	64	63	58.7	83.8
24	08NE114	HIDDEN CREEK NEAR THE MOUTH	68	54	40	7	37	49	79	89	51	51	73	73	58.0	83.7
25	08LG016	PENNASK CREEK NEAR QUILCHENA	79	67	46	3	20	59	80	88	41	28	55	74	54.7	83.6
26	08NL038	SIMILKAMEEN RIVER NEAR HEDLE	42	53	39	15	43	51	80	87	50	38	42	55	51.4	83.5
27	08NM172	PEARSON CREEK NEAR THE MOUT	0	88	33	13	7	9	77	90	67	43	50	63	47.7	83.5
28	08NJ013	SLOCAN RIVER NEAR CRESCENT VA	83	68	46	13	32	53	68	97	62	68	58	80	61.6	82.7
29	08NK002	ELK RIVER AT FERNIE	42	57	33	18	32	46	81	84	84	82	68	59	59.5	82.7
30	08NG065	KOOTENAY RIVER AT FORT STEELE	71	63	60	13	29	53	76	89	70	75	68	64	62.1	82.6
31	08NG076	MATHER CREEK BELOW HOULE CR	78	54	39	21	50	45	84	81	66	61	58	70	60.7	82.3
32	08HB023	ASH RIVER BELOW MORAN CREEK	42	65	58	58	54	74	87	77	52	31	55	39	58.7	82.1
33	08NN023	BURRELL CREEK ABOVE GLOUCEST	70	70	28	8	39	27	73	91	37	31	43	49	48.0	82.1
34	08NG077	ST. MARY RIVER BELOW MORRIS	82	55	55	17	47	36	76	86	35	70	60	51	56.0	81.1
35	08JB003	NAUTLEY RIVER NEAR FORT FRASE	65	83	51	9	50	68	70	91	95	63	63	67	66.3	80.5
36	08HB034	NANAIMO RIVER NEAR CASSIDY	42	55	56	56	63	65	74	87	35	47	37	32	54.5	80.2
37	08LB024	FISHTRAP CREEK NEAR MCLURE	61	67	42	31	79	74	76	84	64	72	55	67	66.7	80.1
38	08NL076	EWART CREEK NEAR CATHEDRAL P	87	83	69	4	27	49	72	88	59	60	74	84	63.6	80.1
39	08MF068	COQUIHALLA RIVER ABOVE ALEXA	52	72	47	36	53	55	80	80	49	37	62	68	58.6	80.1
40	08NH016	DUCK CREEK NEAR WYNNDEL	87	67	55	25	30	42	79	81	82	54	80	90	65.3	80.0
41	08LB020	BARRIERE RIVER AT THE MOUTH	64	62	28	9	31	39	75	85	48	61	54	64	52.9	80.0
42	08NL007	SIMILKAMEEN RIVER AT PRINCETO	48	65	56	9	46	38	81	79	55	44	47	47	52.5	80.0
43	08GA047	ROBERTS CREEK AT ROBERTS CREE	44	50	47	59	64	52	79	81	34	39	41	36	52.5	80.0
44	08LG010	COLDWATER RIVER NEAR MERRIT	39	45	47	22	46	47	77	83	23	39	45	36	46.9	79.8
45	08HB022	NILE CREEK NEAR BOWSER	53	54	73	57	72	65	84	75	41	54	53	30	59.6	79.5
46	08LG048	COLDWATER RIVER NEAR BROOKM	56	71	48	16	39	39	77	81	29	35	47	56	50.3	79.1
47	08FB006	ATNARKO RIVER NEAR THE MOUT	89	78	67	7	24	58	66	92	62	62	66	67	61.8	79.0
48	08NL004	ASHNOLA RIVER NEAR KEREMEOS	46	54	39	4	29	54	75	83	66	63	55	68	55.4	79.0
49	08NN003	WEST KETTLE RIVER AT WESTBRID	44	50	13	15	51	36	68	89	46	48	59	45	49.1	78.7
50	08NH007	LARDEAU RIVER AT MARBLEHEAD	93	67	42	7	25	57	62	95	54	81	71	83	62.2	78.6

Table 6. Top 50 stations ELF Model has largest Jul + Aug percent of accurate forecasts for water levels (Note: RK – rank, ANN – annual, JL+AG – July and August).

	STATION		PERCENT (%) OF ELF MODEL ACCURATE FORECASTS FOR WATER LEVELS													
RK	ID	STATION NAME	JAN	FEB	MAR	APR	MAY	JUN	JUL	AUG	SEP	OCT	NOV	DEC	ANN	JL+AG
1	08MH156	PEPIN CREEK AT INTERNATIONAL B	0	0	0	0	79	73	100	100	100	57	50	63	69.3	100.0
2	08MH029	SUMAS RIVER NEAR HUNTINGDON	38	50	56	100	93	46	100	100	11	100	50	41	65.3	100.0
3	08NM084	SKAHA LAKE AT OKANAGAN FALLS	100	98	98	87	94	83	98	99	94	100	100	100	95.9	98.3
4	08NM143	KALAMALKA LAKE AT VERNON PUM	100	100	98	78	68	92	93	100	96	97	100	100	93.7	96.7
5	07ED001	NATION RIVER NEAR FORT ST. JAM	0	25	22	0	0	9	92	100	89	29	20	38	39.3	96.2
6	08HD021	QUINSAM RIVER AT ARGONAUT BF	85	83	97	56	78	91	95	97	90	51	69	60	79.8	95.9
7	08MH005	ALOUETTE RIVER NEAR HANEY	54	67	75	58	67	70	95	97	78	66	49	63	71.2	95.9
8	08EC003	BABINE LAKE AT TOPLEY LANDING	100	82	91	38	40	70	90	99	93	100	99	100	84.1	94.4
9	08NP003	HOWELL CREEK ABOVE CABIN CREE	68	53	49	13	35	60	100	89	95	52	57	82	65.5	94.3
10	08HA009	COWICHAN LAKE NEAR LAKE COWI	37	52	67	66	88	95	87	95	55	42	55	40	66.1	90.8
11	08NK002	ELK RIVER AT FERNIE	44	52	30	36	49	49	85	96	88	83	68	51	63.2	90.3
12	08NL076	EWART CREEK NEAR CATHEDRAL PA	98	87	92	33	50	66	81	99	84	88	95	97	81.2	89.9
13	08NE039	BIG SHEEP CREEK NEAR ROSSLAND	68	44	29	26	47	69	82	97	54	51	64	59	59.7	89.6
14	08NK022	LINE CREEK AT THE MOUTH	71	61	82	32	35	59	92	86	100	91	77	67	73.4	89.4
15	08NL069	PASAYTEN RIVER ABOVE CALCITE C	68	75	58	21	58	42	81	97	73	64	54	22	60.5	88.9
16	08NM083	OKANAGAN LAKE AT KELOWNA	100	83	86	40	38	77	80	97	100	97	99	100	83.7	88.8
17	08JB003	NAUTLEY RIVER NEAR FORT FRASE	75	90	58	24	67	74	80	97	96	70	70	75	74.6	88.8
18	08NE130	WHATSHAN RIVER BELOW BARNES	0	50	0	13	14	18	77	100	33	57	40	50	41.1	88.5
19	08NG002	BULL RIVER NEAR WARDNER	67	73	44	22	53	53	80	96	84	76	79	85	69.6	88.1
20	08NE114	HIDDEN CREEK NEAR THE MOUTH	70	58	36	29	52	55	79	97	60	59	66	79	63.7	87.7
21	08EC001	BABINE RIVER AT BABINE	90	100	93	24	38	66	87	88	89	75	80	87	76.8	87.4
22	08ME029	BRIDGE RIVER BELOW LAJOIE DAM	65	74	72	68	39	75	90	84	31	55	87	98	70.1	87.3
23	08MG001	CHEHALIS RIVER NEAR HARRISON	53	50	56	50	36	36	85	90	75	43	50	76	60.1	87.3
24	08NK030	ELK RIVER BELOW ELKO DAM	75	57	61	35	44	52	80	93	89	85	75	73	69.6	86.8
25	08MF068	COQUIHALLA RIVER ABOVE ALEXAN	62	67	56	44	49	57	82	91	54	44	55	77	62.3	86.6
26	08MF062	COQUIHALLA RIVER BELOW NEEDL	65	65	73	23	47	46	81	92	41	25	58	71	58.1	86.6
27	08JB007	NADINA LAKE NEAR NORALEE	100	90	84	40	53	79	84	89	78	68	78	84	77.3	86.4
28	08HA001	CHEMAINUS RIVER NEAR WESTHO	44	63	67	71	76	78	84	89	39	39	61	45	63.6	86.4
29	08HA016	BINGS CREEK NEAR THE MOUTH	52	63	74	86	96	77	91	81	52	39	52	39	67.2	86.3
30	08LG008	SPIUS CREEK NEAR CANFORD	80	69	82	51	44	65	79	93	75	65	63	78	70.6	85.8
31	08HA002	COWICHAN RIVER AT LAKE COWICH	35	55	72	56	51	47	77	95	50	27	61	43	56.3	85.8
32	08HB022	NILE CREEK NEAR BOWSER	62	55	63	64	76	70	91	80	45	59	58	39	64.0	85.4
33	08HD025	WOKAS LAKE NEAR CAMPBELL RIVE	44	59	70	40	43	66	75	96	84	48	47	72	63.5	85.4
34	08LG016	PENNASK CREEK NEAR QUILCHENA	85	76	54	19	37	63	80	91	53	38	55	75	61.4	85.4
35	08MH155	NICOMEKL RIVER AT 203 STREET L	50	70	63	69	75	75	89	81	56	41	44	44	63.8	85.2
36	08GE003	ICY CREEK NEAR THE MOUTH	83	80	74	49	71	69	97	73	79	76	69	77	75.5	85.0
37	08MH168	OR CREEK NEAR COQUITLAM	50	68	65	75	62	73	85	85	52	65	62	60	67.4	85.0
38	08HD018	ELK RIVER ABOVE CAMPBELL LAKE	58	68	60	60	65	70	85	85	52	51	58	72	66.1	85.0
39	08NL007	SIMILKAMEEN RIVER AT PRINCETO	56	70	58	18	58	48	85	85	61	58	42	47	58.5	85.0
40	10AA006	LIARD RIVER BELOW SCURVY CREE	0	0	88	25	14	36	100	70	22	43	20	93	48.7	85.0
41	08NM037	SHATFORD CREEK NEAR PENTICTOI	90	80	49	25	46	52	80	89	56	62	81	83	66.7	84.8
42	08NJ160	LEMON CREEK ABOVE SOUTH LEMC	64	63	53	16	35	49	80	89	60	58	61	73	59.8	84.8
43	08HB023	ASH RIVER BELOW MORAN CREEK	52	67	75	64	64	77	88	81	56	39	59	49	64.9	84.6
44	08NL038	SIMILKAMEEN RIVER NEAR HEDLEY	50	55	44	18	47	51	78	91	49	41	39	59	53.3	84.4
45	08NJ026	DUHAMEL CREEK ABOVE DIVERSIO	85	65	30	27	53	46	82	85	63	59	55	84	62.4	83.9
46	08LE108	EAST CANOE CREEK ABOVE DAM	68	75	39	13	67	79	77	90	69	65	57	88	68.6	83.8
47	08HF004	TSITIKA RIVER BELOW CATHERINE	63	67	60	58	73	71	79	89	57	53	64	64	67.1	83.7
48	08NH139	MOYIE RIVER ABOVE NOKE CREEK	89	63	52	8	50	54	96	71	56	36	72	67	62.1	83.6
49	08GC007	THEODOSIA RIVER BELOW OLSEN L	69	63	54	39	54	63	86	81	45	62	61	68	63.2	83.5
50	08NK016	ELK RIVER NEAR NATAL	65	69	56	12	38	59	79	87	96	93	54	65	66.6	82.9

Table 7 shows the statistics of numbers of stations, for which the ELF Model has accurate forecasts of discharge and water level equal to and greater than 50%, 60%, 70%, 80% and 90%, from January to December and the entire year. Figure 13 (a) and (b) are bar charts of Table 7 for the forecasts of discharge and water level. From Table 7 and Figure 13, it can be seen that generally July and August are the two months that there are the largest numbers of stations that the ELF Model has large percents (>=50 to 90%) of accurate forecasts. And on the contrary, April and May are the two months that there are the least numbers of stations that the ELF Model has large percents (>=50 to 90%) of accurate forecasts. Other months of year are in between with respect to numbers of stations that the ELF Model has large numbers of accurate forecasts. This means that the droppings of streamflow at more stations in most time of July and August follow the trends governed by Equations (15) and (16) given in Section 5 and (30) and (31) given in Section 7, and the streamflows in these two months fulfill the fundamental assumption for mathematical methods for low flow simulation described in Section 4.

It also can be seen from Tabel 3 and Figure 13 that the number of stations that the ELF Model forecasts of water level with accurate forecasts is larger than the number of stations that the ELF Model forecasts of discharge with accurate forecasts. Or in simple words, the ELF Model forecasts of water level have higher accuracy than forecasts of discharge. The reason for this may be that the data quality of discharges is lower than that of water levels in the low flow period as stated on page 39.

Table 7. Statistics of numbers of stations with accurate forecasts equal to and greater than 50 to 90%

	NUMBERS OF STATIONS WITH ACCURATE FORECASTS >= 50 TO 90%									
	FORECASTS OF DISCHARGE					FORECASTS OF WATER LEVEL				
Month	>=90%	>=80%	>=70%	>=60%	>=50%	>=90%	>=80%	>=70%	>=60%	>=50%
JAN	18	55	124	198	282	23	64	123	213	306
FEB	11	50	116	214	318	16	41	116	242	356
MAR	7	20	50	109	219	11	24	64	153	253
APR	4	5	11	30	67	2	7	23	64	100
MAY	3	6	23	53	108	5	19	56	101	169
JUN	0	5	24	110	237	5	14	58	149	293
JUL	9	40	132	256	338	18	67	169	281	358
AUG	37	95	165	261	332	44	110	199	296	366
SEP	18	36	67	145	246	19	50	90	165	280
OCT	3	16	69	142	215	10	32	78	175	267
NOV	10	26	76	166	278	12	31	87	195	319
DEC	12	49	108	206	277	14	52	126	213	309
ANN	0	0	6	78	301	2	6	23	143	338

Note: There was a total of 439 stations in ELF Model in 2022.

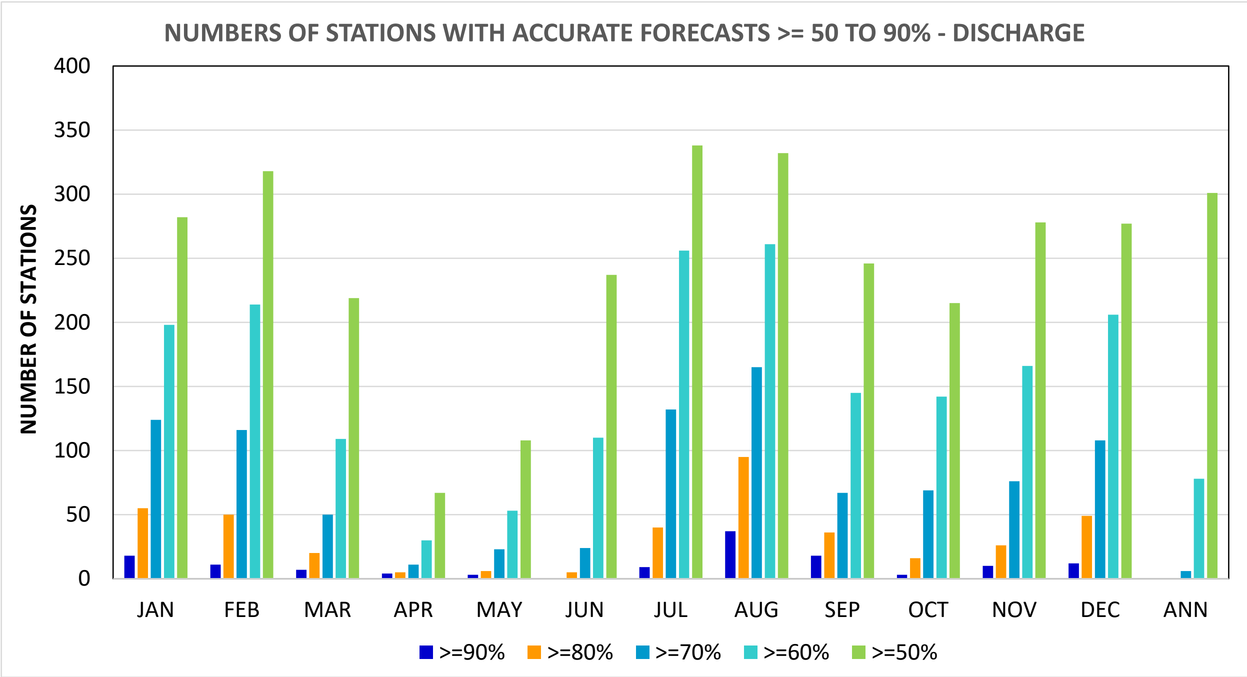

(a) Forecasts of discharge

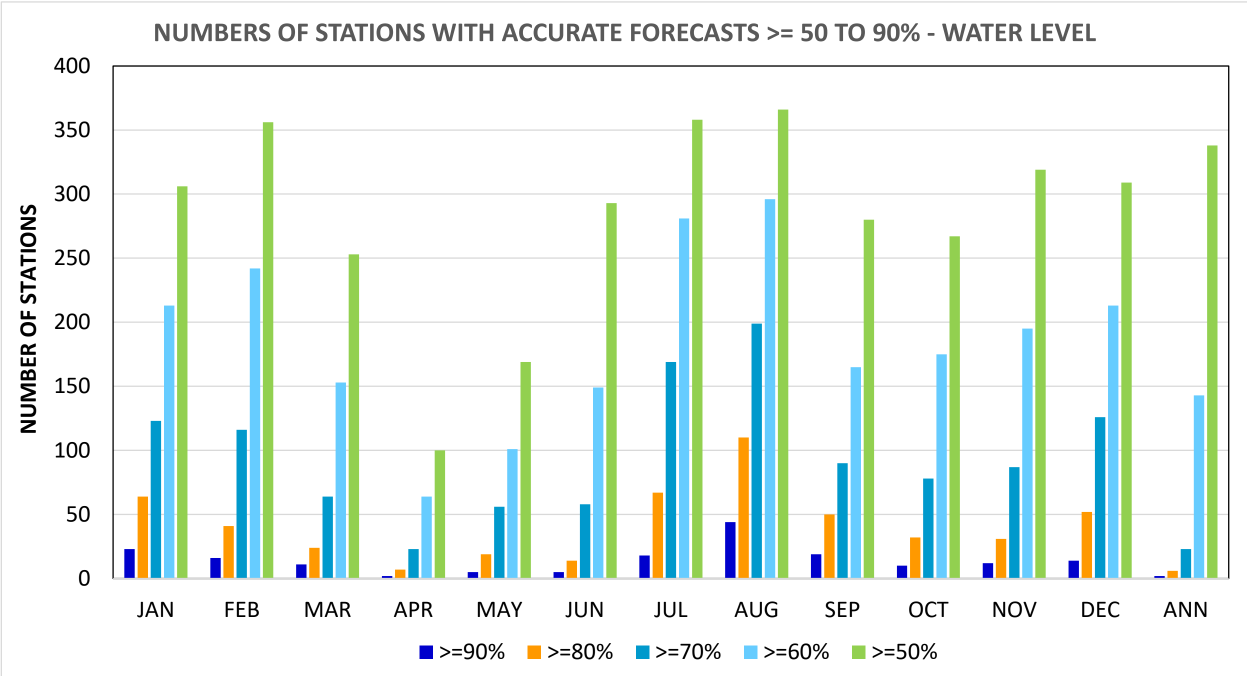

(b) Forecasts of water level

Figure 13. Statistical bar charts of numbers of stations with accurate forecasts equal to and greater than 50 to 90%

10. Forecasts of rise

The ELF Model is run all year round using 30 day observed flow data (discharges and/or water levels) to produce forecasts for the next 30 days regardless the flow is rising or dropping. Sometimes the forecasts of rise are very accurate (Figure 14). These forecasts of rise are for information only and are not recommended for management purposes because the ELF Model is not developed for forecasting rises and because the model has no meteorological data input.

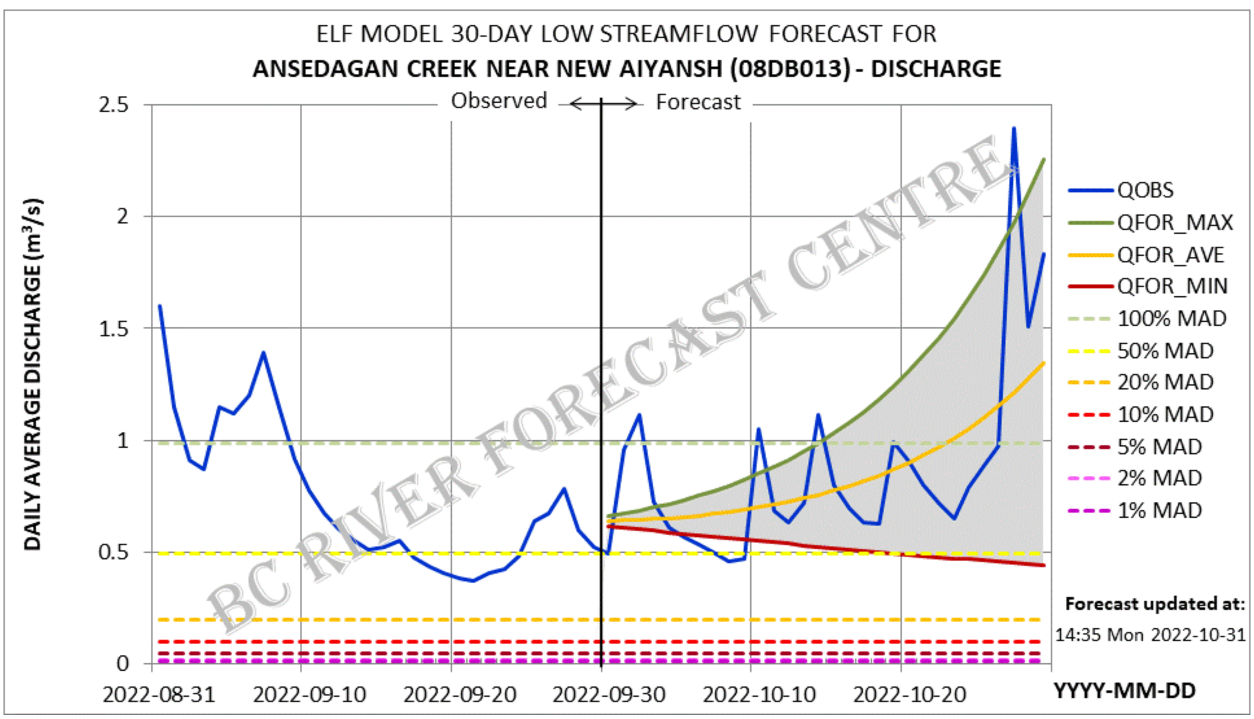

(a) Forecast of rise for discharge – ANSEDAGAN CREEK NEAR NEW AIYANSH (08DB013)

Figure 14. Examples of ELF Model accurate forecasts of rise (continued on next page.)

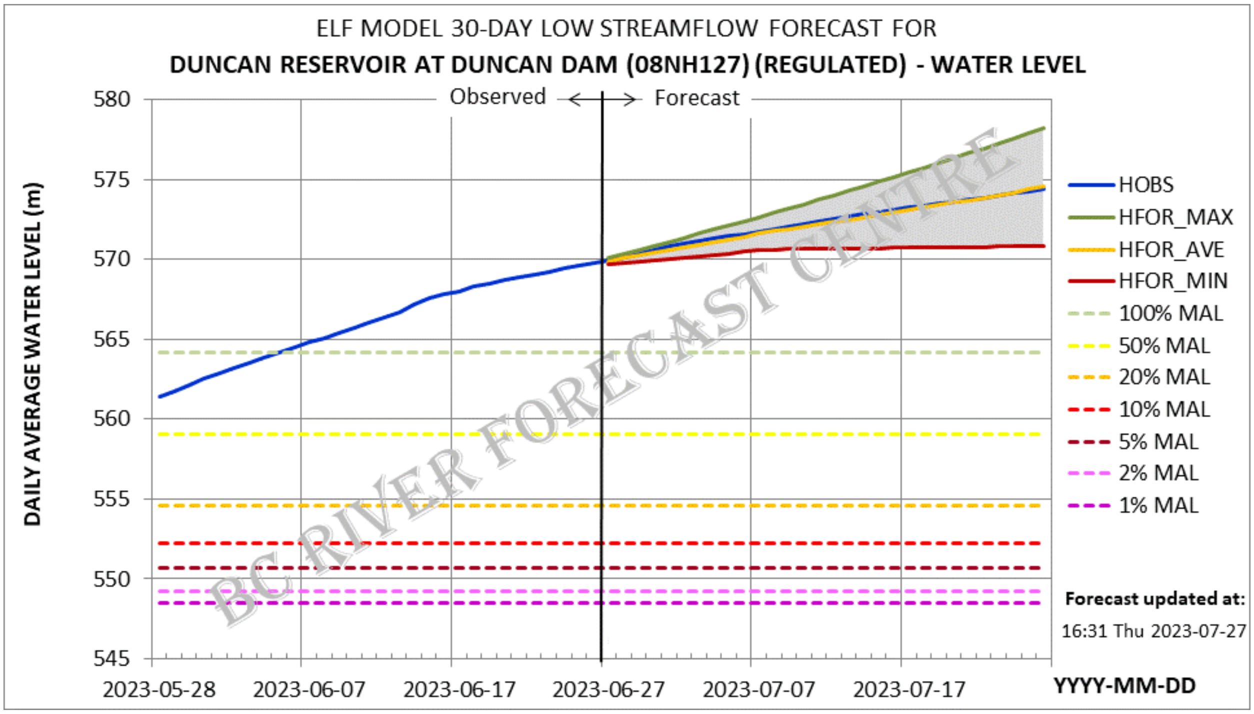

(b) Forecast of rise for water level – DUNCAN RESERVOIR AT DUNCAN DAM (08NH127)

Figure 14. Examples of ELF Model accurate forecasts of rise (continued.)

11. Forecasts for regulated stations

The regulated flow stations are not removed from the list of modeled stations. As such, the ELF Modal also produce forecasts for the regulated stations and sometimes the forecasts are also accurate as long as the operation of the regulating facilities is consistent during the period of the model’s input data and the period of forecasting (Figure 15). These forecasts are also for information only and are not recommended for management purpose either because the forecast accuracy is uncertain.

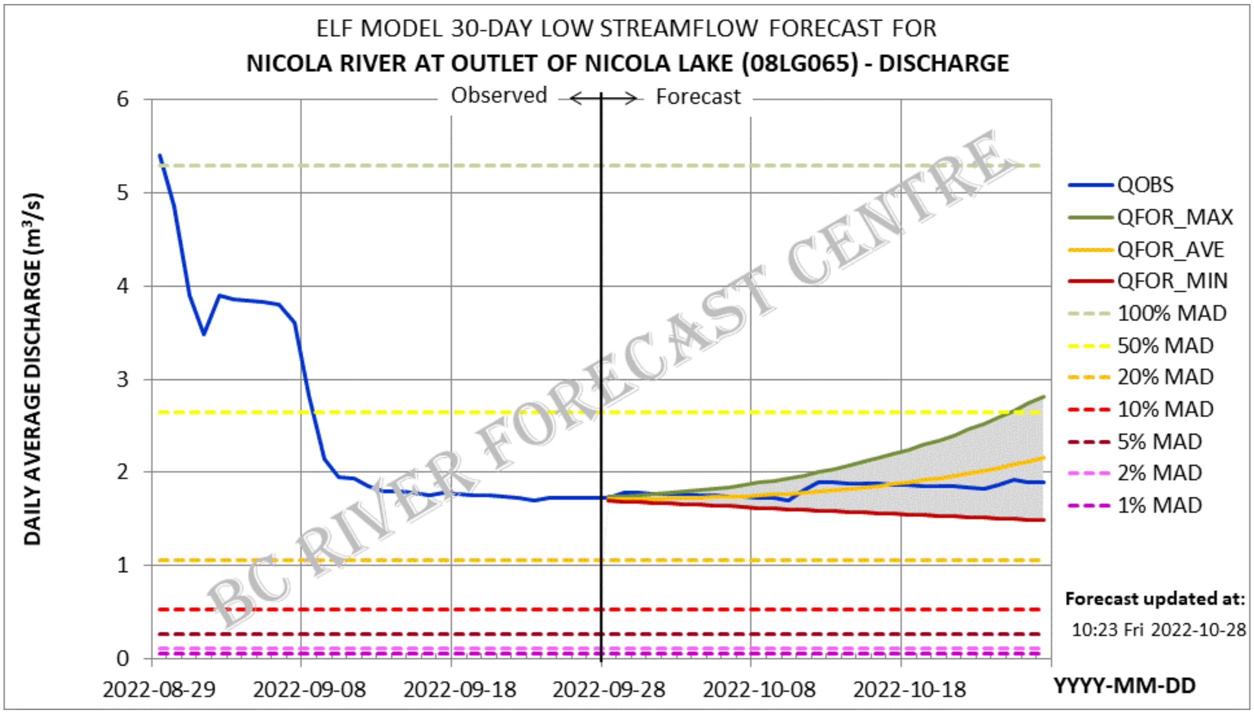

(a) Forecast for regulated station – NICOLA RIVER AT OUTLET OF NICOLA LAKE (08LG065)

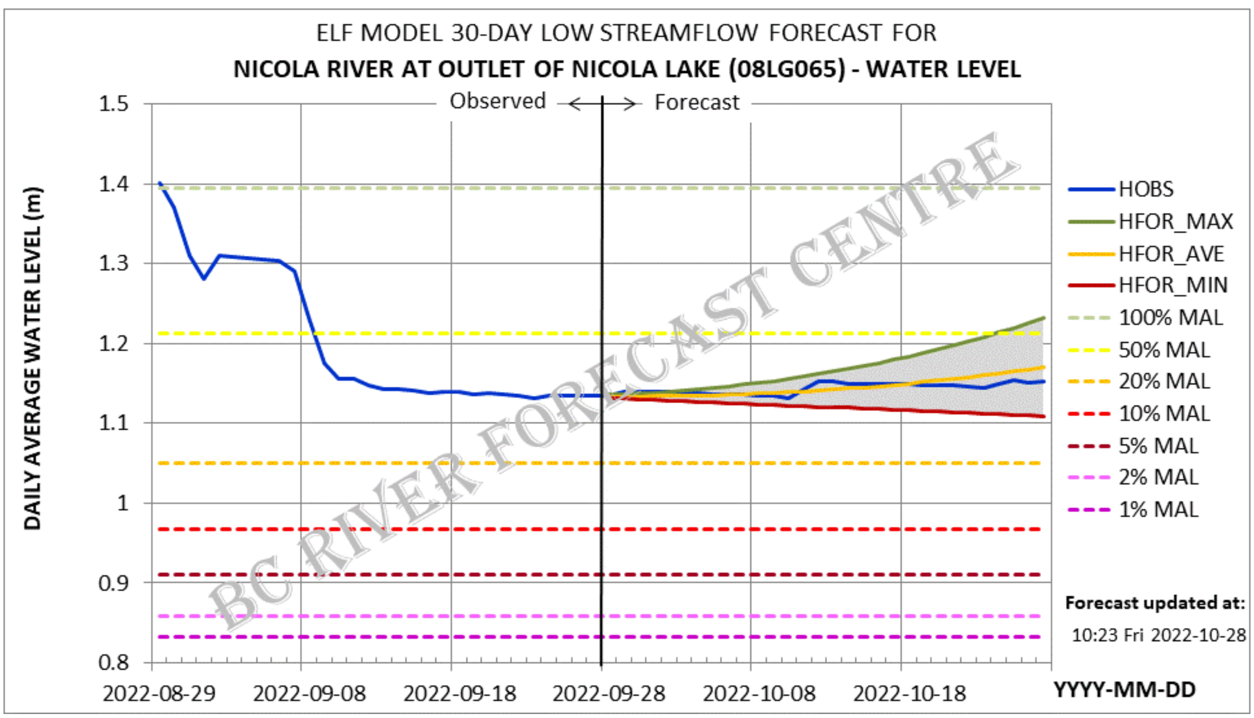

(b) Forecast for regulated station – NICOLA RIVER AT OUTLET OF NICOLA LAKE (08LG065)

Figure 15. Examples of ELF Model accurate forecasts for regulated stations

12. Summary and conclusions

British Columbia (BC) experienced drought hazards in the history, and the memory of drought in BC continues to be refreshed in the recent years. The River Forecast Centre (RFC) is part of BC provincial drought responding resources and low flow forecasting for drought managements is within its responsibilities. On this background, the ELF Model was developed in the RFC for medium-term (30 days) low flow forecasting in BC.

In this study, the low flow is redefined from the hydrological perspective as “the outflow from a watershed that has been continuously decreasing from the most recent high peak for a period.” The decreasing period is called the “receding period,” which can be determined from the historical flow data. With this definition and the receding period, the low flow is more predictable under climate change. Based on this definition, the characteristics of low flow can be summarized as that, (1) the streamflow is decreasing, (2) the sum of the rate of release from the watershed liquid water storage plus the rate of net meteorological liquid water input is decreasing, (3) the net meteorological liquid water input is not sufficient to replenish the liquid water storage in the watershed, (4) the watershed liquid water storage is decreasing.

Hydrological methods for low flow simulation are faced with the following three obstacles: (1) The magnitude of low flow is very small and sometimes is about the magnitudes of measurement errors or forecast errors of any hydrological model. (2) “Low flow” is always referred to as “baseflow” in hydrological models. For most conceptual/ lumped-sum hydrological models, the baseflow is a preset constant. Consequently, the changing low flow cannot be simulated with a conceptual/ lumped-sum hydrological model. (3) For physically based distributed hydrological models, the baseflow is mainly from the release of groundwater. Severe insufficiency of groundwater and aquifer data prevent this kind of hydrological models to generate accurate low flow forecasts.

In order to avoid the obstacles faced by hydrological methods in low flow simulation, mathematical or empirical methods are an inevitable alternative. In this study, the fundamental assumption for mathematical methods for low flow forecasting is that the sum of the water release rate from the watershed liquid water storage plus the net meteorological liquid water input rate to the streamflow is a function of time and parameters, and the parameters remain constant for a certain period.

The basic equation for the mathematical method is the exponential recession equation. The first order and second order derivatives for discharge and water level with respect to time are derived. Based on these derivative equations, the first characteristic of low flow is extended to that the streamflow is decreasing, and the decreasing rate of the streamflow becomes smaller and smaller with time.

In this study, the ELF Model uses 30-day of logarithmic streamflow data to produce 30-day of forecasts. There are only two parameters in the linear logarithmic equation, and therefore the system becomes overdetermined if all the 30 data points are fitted in the linear equation at once. The least squares method is employed to find the two parameters of the linear logarithmic equation for the overdetermined system.

In the real world, the actual low flow data may include significant noises, and the logarithmic flow may not always be linear. In this study, the so-called “twelve-step and twelve-scenario scheme” is developed to meet the challenges posed by the data noise and non-logarithmic flow issues. This scheme also produces analogues to ensemble forecasts for low flows, which include forecast maximums, minimums, and averages for the next 30 days. In a run, the ELF Model generates a series of products, (1) a Maphub GIS map with color coded markers, (2) interactive charts of forecast hydrographs for discharges and water levels, (3) static charts of forecast hydrographs for discharges and water levels, (4) forecast verifications for the previous month and a similar period of the previous year, and (5) text (csv) files of the daily forecasts.

In this study, a different approach is employed to evaluate the model forecast accuracy – how the forecast maximums and the minimums accommodate the observed flows, (1) the forecast is first said accurate if all the observed flows (daily discharges or water levels) fall in between the forecast maximums and minimums in the 30-day forecasting period, (2) 2/3 of the observed data points fall in between the forecast maximums (+10%) and minimums (-10%), (3) 1/3 of the observed data points, which are the lowest in the forecasting period, fall in between the forecast maximums (+10%) and minimums (-10%), or (4) 3/5 of the last 5 observed data points in the forecasting period fall in between the forecast maximums (+10%) and minimums (-10%).

The ELF Model was put into operation as of July 2018, and together with the reconstructed “forecasts” from January 2015 to June 2018, there is a total of 8 years of forecasts by the end of 2022 (about 800) for each of the 439 stations. A statistical analysis for the ELF Model historical forecasts for all the flow stations was carried out. Bar charts of percents of accurate forecasts of discharges and water levels for each month and the entire year are plotted for all the modeled stations based on the statistical analysis results. The results show that, in general, the ELF Model has better forecasts for most stations in July and August than in the other months, the forecast accuracy is the lowest in April and May, and the forecast accuracy for water levels is higher than that for discharges.

The ELF Model is run all year round and sometimes also forecasts rises. The ELF Model does not exclude the regulated stations from the forecasts. However, these forecasts are for information only though they may be accurate sometimes.

From the findings of his study, it can be concluded that (1) the definition of low flow in this study makes low flows more predictable under climate change, (2) the “twelve-step and twelve-scenario scheme” developed in this study is an effective scheme to meet the challenges posed by the data issues, and produces analogues to ensemble forecasts for low flows, and (3) the statistical analysis results indicate that the ELF Model can produce accurate low flow forecast when the streamflow conditions fulfill the fundamental assumption for mathematical methods for low flow simulation and fulfill the exponential recession equation during the model input data and forecasting periods.

13. References

BC Gov., 2023 a. "Historical British Columbia Drought Information" in British Columbia Drought Information Portal, https://governmentofbc.maps.arcgis.com/apps/MapSeries/index.html?appid=838d533d8062411c820eef50b08f7ebc (Accessed on April 19, 2023.)

BC Gov., 2023 b. "BC Groundwater Wells and Aquifers" https://apps.nrs.gov.bc.ca/gwells/aquifers?map_centre=53.810684,-124.817461 (Accessed on August 3, 2023.)

Barnes, B.S., 1939. "The structure of discharge recession curves." Trans. AGU 20, 721-725.

Bonsal, B. R., E. Wheaton, A. C. Chipanshi , C. A. Lin, D. J. Sauchyn, and L. Wen, 2011. "Drought research in Canada: A review." Atmos. – Ocean, 49, 303–319, doi:10.1080/07055900.2011.555103. https://www.tandfonline.com/doi/full/10.1080/07055900.2011.555103 (Accessed on April 18, 2023.)

Demirel, M. C., Booij, M. J., and Hoekstra, A. Y., 2015. "The skill of seasonal ensemble low flow forecasts in the Moselle River for three different hydrological models." Hydrol. Earth Syst. Sci., 19, 275–291, https://doi.org/10.5194/hess-19-275-2015.

Econnics and MOE (British Columbia Ministry of Environment), 2015. British Columbia Drought Response Plan. https://www.summerland.ca/docs/default-source/works-and-utilities/bc-drought-response-plan.pdf?sfvrsn=0 (Accessed on April 18, 2023.)

Gustard, A., 1983. "Regional variability of soil characteristics for flood and low flow estimation." Agricultural Water Management, 6(2-3), 255-268.

Gustard, A., A. Bullock and J.M. Dixon, 1992. "Low Flow Estimation in the United Kingdom." Report No. 108, Institute of Hydrology, Crowmarsh Gifford, Wallingford, Oxfordshire, United Kingdom, pp88. https://nora.nerc.ac.uk/id/eprint/6050/1/IH_108.pdf (Accessed on July 5, 2023.)

Hall, F.R., 1968. "Base-flow recession - A review." Water Resources Research. 4 (5), 973-983.

Luo, Q., 2000 a. "Non-optimization direct method of inverse problem (NODMIP) for groundwater modeling in a large-scale basin," J. Japan Soc. Hydrol. & Watger Resour., 13(2), 148-155.

Luo, Q., 2000 b. "Chapter 7 Groundwater Models" in "A Distributed Water Balance Model in Large -scale Complex Watersheds (LCW) and Its Application to the Kanto Region." Ph.D. dissertation of the University of Tokyo, Tokyo, Japan, September 2000, pp.152.

Luo, Q., 2007. "A distributed surface flow model for watersheds with large water bodies and channel loops," Journal of Hydrology 337, 172–186.

Luo, C., 2015. Technical reference for the CLEVER model—A real-time flood forecasting model for British Columbia. BC River Forecast Centre, Victoria, BC, Canada.

Luo, C., 2021. “Comparing five kinematic wave schemes for open-channel routing for wide-tooth-comb-wave hydrographs,” J. Hydrol. Eng., 26(4). DOI: 10.1061/(ASCE)HE.1943-5584.0002079.

MEKIS, E. and L.A. VINCENT. 2008. “Changes in daily and extreme temperature and precipitation indices related to droughts in Canada.” In Proc. 17th Applied Climatology Conference. Whistler, BC.

Nicolle, P., Pushpalatha, R., Perrin, C., François, D., Thiéry, D., Mathevet, T., Le Lay, M., Besson, F., Soubeyroux, J.-M., Viel, C., Regimbeau, F., Andréassian, V., Maugis, P., Augeard, B., and Morice, E., 2014. “Benchmarking hydrological models for low flow simulation and forecasting on French catchments,” Hydrol. Earth Syst. Sci., 18, 2829–2857, https://doi.org/10.5194/hess-18-2829-2014.

Quick, M.C. and Pipes, A., 1977. “U.BC Watershed Model.” Hydrological Sciences Bulletin, 22:1, 153-161.

Reed, D. W., and D. W. Warne, 1985. "Low flow forecasting to aid regulation of the river Wye." Technical Report of Institute of Hydrology, Natural Environment Research Council, UK, http://nora.nerc.ac.uk/id/eprint/14798/1/N014798CR.pdf (Accessed on April 18, 2023.)

Risva, K., Nikolopoulos, D., Efstratiadis, A., and Nalbantis, I., 2018. “A Framework for Dry Period Low Flow Forecasting in Mediterranean Streams,” Water Resour. Manag., 32, 4911–4932, https://doi.org/10.1007/s11269-018-2060-z.

Smakhtin, V.U., 2001. "Low flow hydrology: a review." Journal of Hydrology. 147-186.

Szeto, k., X. Zhang, R.E. White, and J. Brimelow, 2016. “9. THE 2015 EXTREME DROUGHT IN WESTERN CANADA,” DOI:10.1175/BAMS-D-16-0147.1, BANS | DECEMBER 2016, S42-S46, http://www.ametsoc.net/eee/2015/9_canada_drought.pdf (Accessed on April 18, 2023.)

Toebes, C., and Strang, D.D., 1964. “On recession curves. 1 - Recession equations.” Hydrol. (NZ) 3 (2), 2-15.

USEPA (United States Environmental Protection Agency), 2022. “Definitions and Characteristics of Low Flows.” https://www.epa.gov/ceam/definition-and-characteristics-low-flows, (Last Updated on August 31, 2022.) (Accessed on August 10, 2023.)

VINCENT, L.A. and E. MEKIS, 2006. “Changes in daily and extreme temperature and precipitation indices for Canada over the twentieth century.” ATMOSPHERE-OCEAN, 44: 177–193.

WLRS (British Columbia Ministry of Water, Land and Resource Stewardship) and IADWG (Inter-Agency Drought Working Group), 2023. British Columbia Drought and Water Scarcity Response Plan, https://www2.gov.bc.ca/assets/gov/environment/air-land-water/water/drought-info/drought_response_plan_final.pdf (Accessed on August 18, 2023.)

WMO (World Meteorological Organization), 2008. “Manual on Low flow Estimation and Prediction,” Operational Hydrology Report No. 50, WMO-No. 1029, pp138. https://library.wmo.int/doc_num.php?explnum_id=7699. (Accessed on June 13, 2023.)